CANFSA

Center for Advanced Non-Ferrous Structural Alloys
An Industry/University Cooperative Research Center

Project 55: Fe-Containing Multi-Principal Element Alloys for Protective Structures

Semi-annual Spring Meeting
April 2022

- Student: James Frishkoff (Mines)
- Faculty: Dr. Amy Clarke & Dr. Kester Clarke (Mines)
- Industrial Mentors: Bruce Antolovich (ATI), Hayley Brown (SFSA), *Steve Jansto (CBMM), Tanya Ros (Arcelor Mittal)*

COLORADO SCHOOL OF MINES · NSF · IOWA STATE UNIVERSITY

Project 55: Fe-Containing Multi-Principal Element Alloys for Protective Structures

CANFSA CENTER FOR ADVANCED NON-FERROUS STRUCTURAL ALLOYS

- Student: James Frishkoff (Mines)
- Advisor(s): Amy Clarke, Kester Clarke (Mines)

Project Duration

PhD: January 2021 to June 2025 (December 2022 current scope)

- Problem: TRIP/TWIP MPEAs currently rely on costly high alloy content, and composition dependence not yet well understood.
- Objective: Achieve TRIP/TWIP & strength-ductility combinations in Co-lean MPEAs via experimental methods and high-throughput thermodynamic modeling.
- Benefit: Increasingly high strength-ductility combinations desired in many sectors, including vehicle protective structures.

Recent Progress

- Alloy downselect completed - 7 1st choice alloys + backups
- Arc melting of bulk samples of selected new alloys
- Design of experiment for microstructure evolution study
- Identified heat treatments for new alloys & ATI baseline alloys
- Characterization of new & baseline alloys initiated

Metrics

Description	% Complete	Status
1. Literature review	70%	●
2. ThermoCalc, PanDat & LAMMPS modeling	85%	●
3. Obtain industrial baseline material	100%	●
4. Alloy downselect	90%	●
5. Gleeble experiments on downselected alloys and industrial reference material	0%	●

Industrial Relevance

- TRIP & TWIP MPEAs may combine high ductility & tensile strength as well as high work-hardening rates
- High strength-ductility combinations correlate to high deformation energy absorption - applications include automotive frames & ballistic protection
- Previous TRIP/TWIP MPEAs rely on cobalt content ≥10%
- Reduction of Co content important to reduce cost
- Mechanical data at varied temperatures, strain rates important for building processing maps; also helps predict high-rate impact behavior

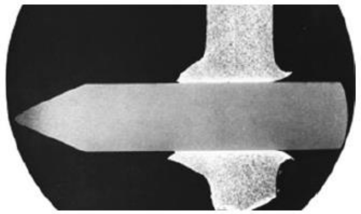
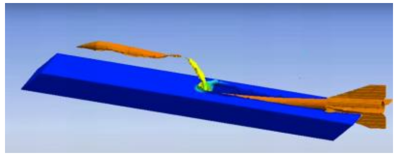
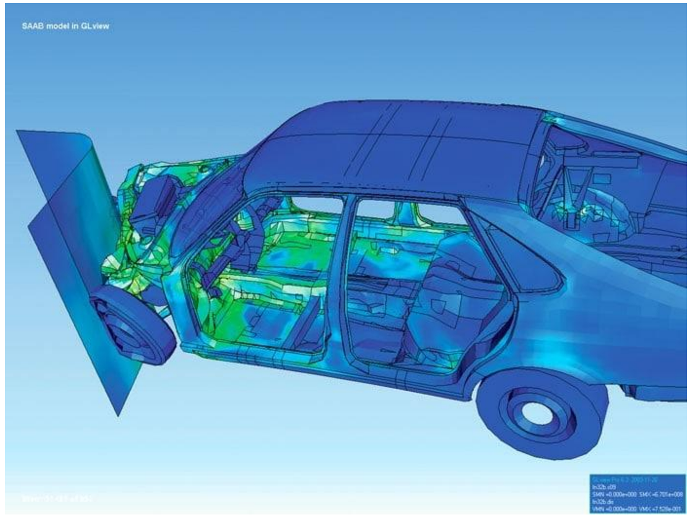

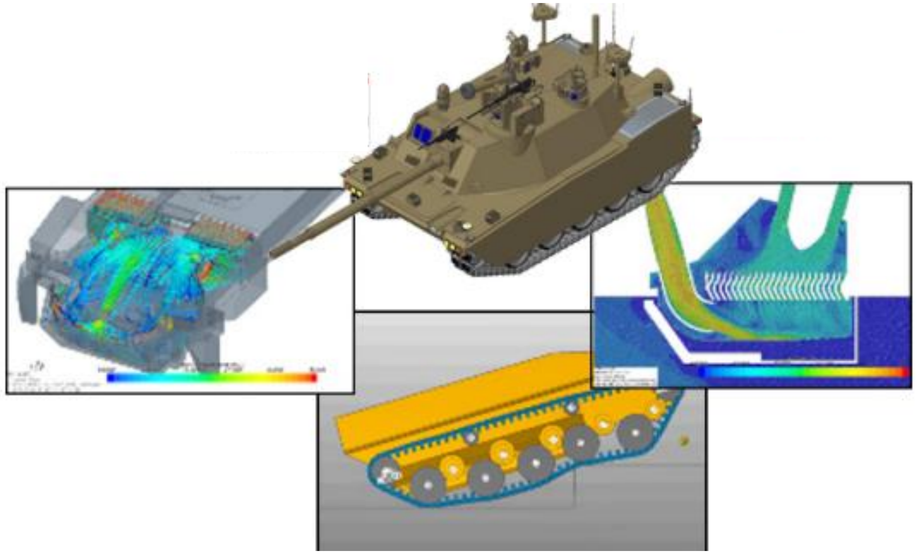


The Problem Space

CANFSA
CENTER FOR ADVANCED NON-FERROUS STRUCTURAL ALLOYS

Problem	Threat	Protection	Solution
Military ground/air platforms need armor/protective structures Platforms are weight-constrained	Increasing lethality of threats requires improved protective capabilities	Protection scales with weight “Weight is the penalty we pay for having nice things”	Higher performance armor materials Better performance at the same weight, or the same performance at a lower weight

Performance Metrics for Protective Structures

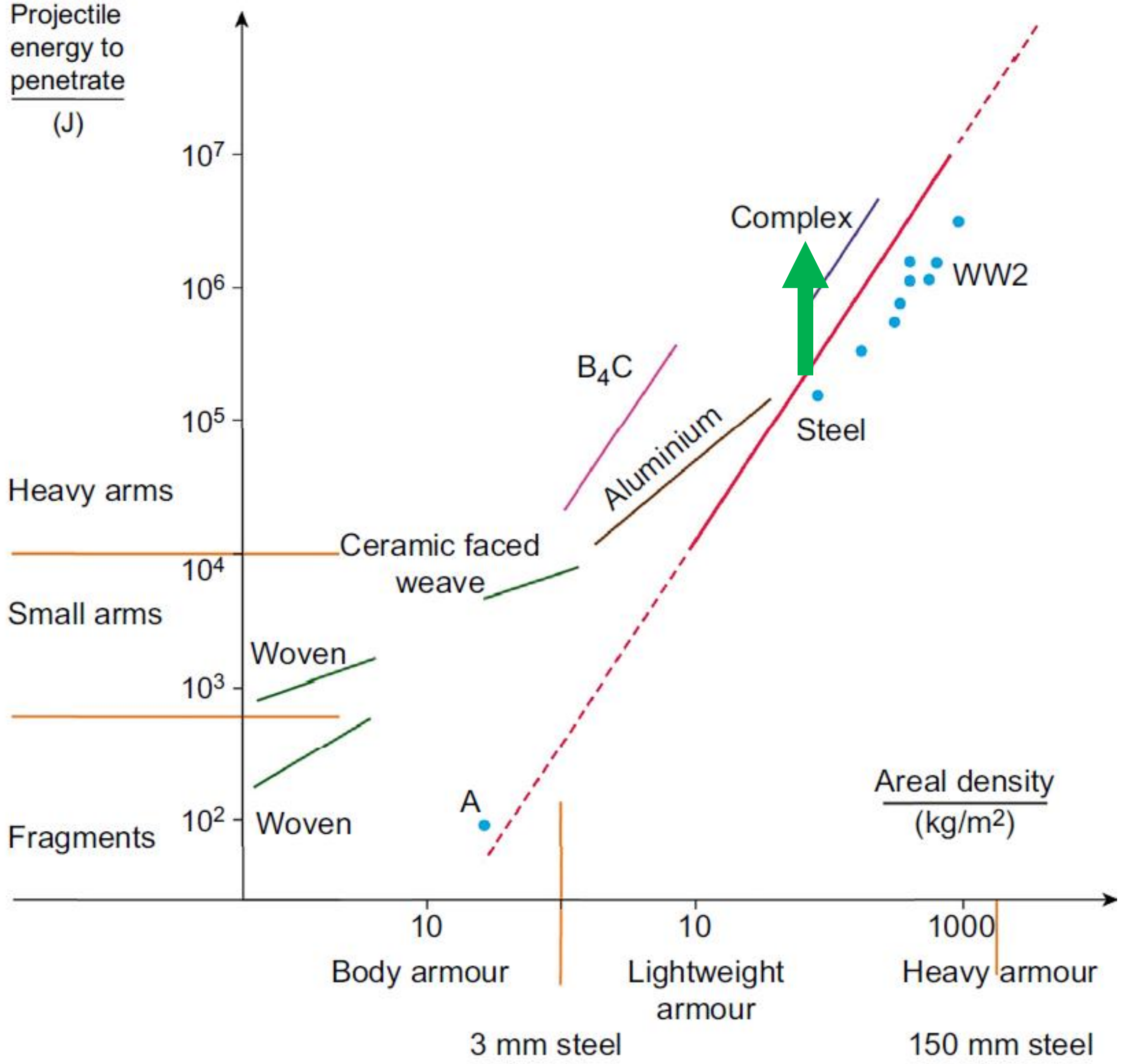

Wants and needs:

- Yield & Dynamic Flow Stress (quasistatic up to 10^4 s^{-1})
- Ultimate Tensile Strength
- Strain to Fracture
- Work Hardening Rate
- Shear Strain Localization Resistance
- Surface Hardness
- Weldability

I. Crouch, *The Science of Armour Materials,* Elsevier (2017). Reproduced from A. Doig, *Military Metallurgy*, Maney Publishing: London (1998)

Steel Example: Austenite/Martensite Mixtures Create Desirable Property Combinations

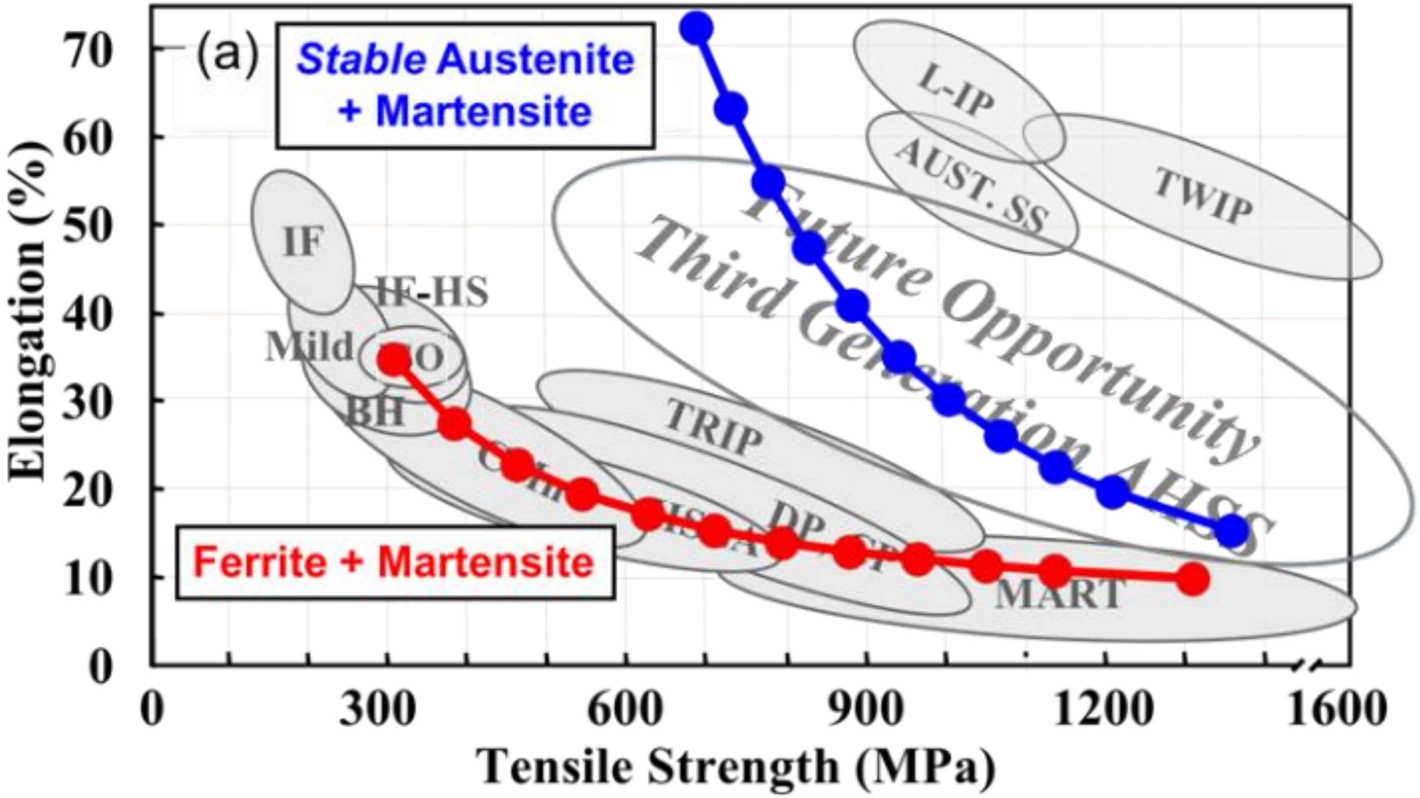

D.K. Matlock and J.G. Speer, *Proceedings of The 3rd International Conference on Advanced Structural Steels*, 2006, pp. 774-781

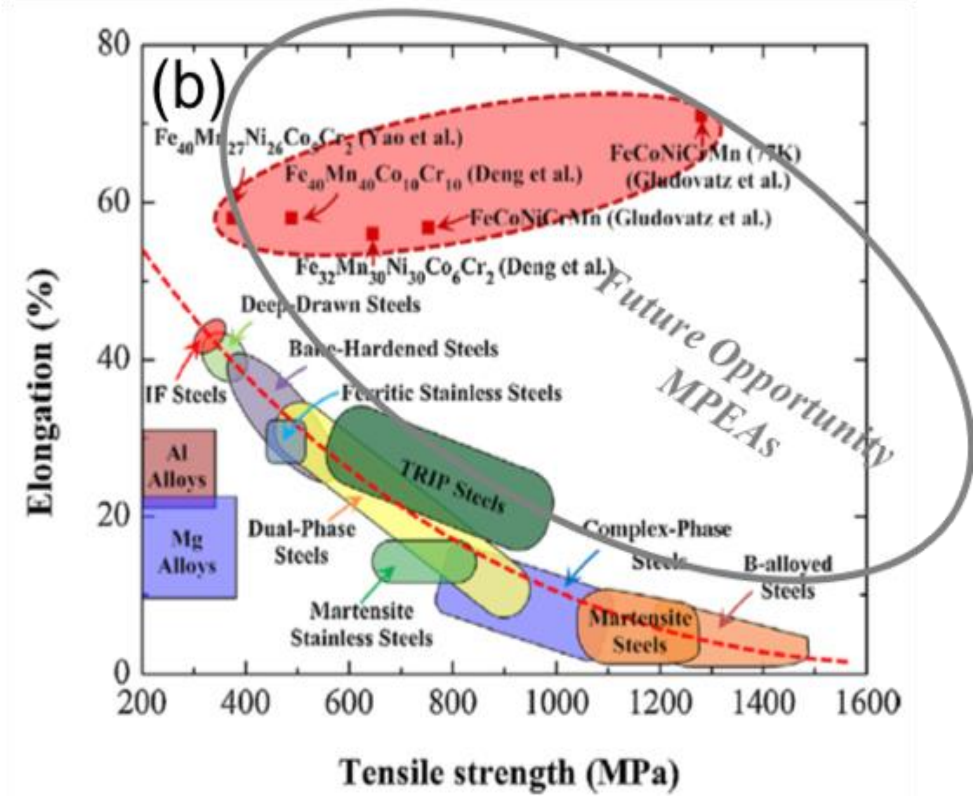

Ye et al, *Materials Today* 2011

Center Proprietary – Terms of CANFSA Membership Agreement Apply

Program Goals & Gates – Year 1

CANFSA
CENTER FOR ADVANCED NON-FERROUS STRUCTURAL ALLOYS

1. **Literature review to guide alloy recipes to be simulated**
2. **Use thermodynamic simulation to design alloys likely to be successful during year 2 trials**
3. **Perform characterization of effect of experimental TMP on Datalloy HP**

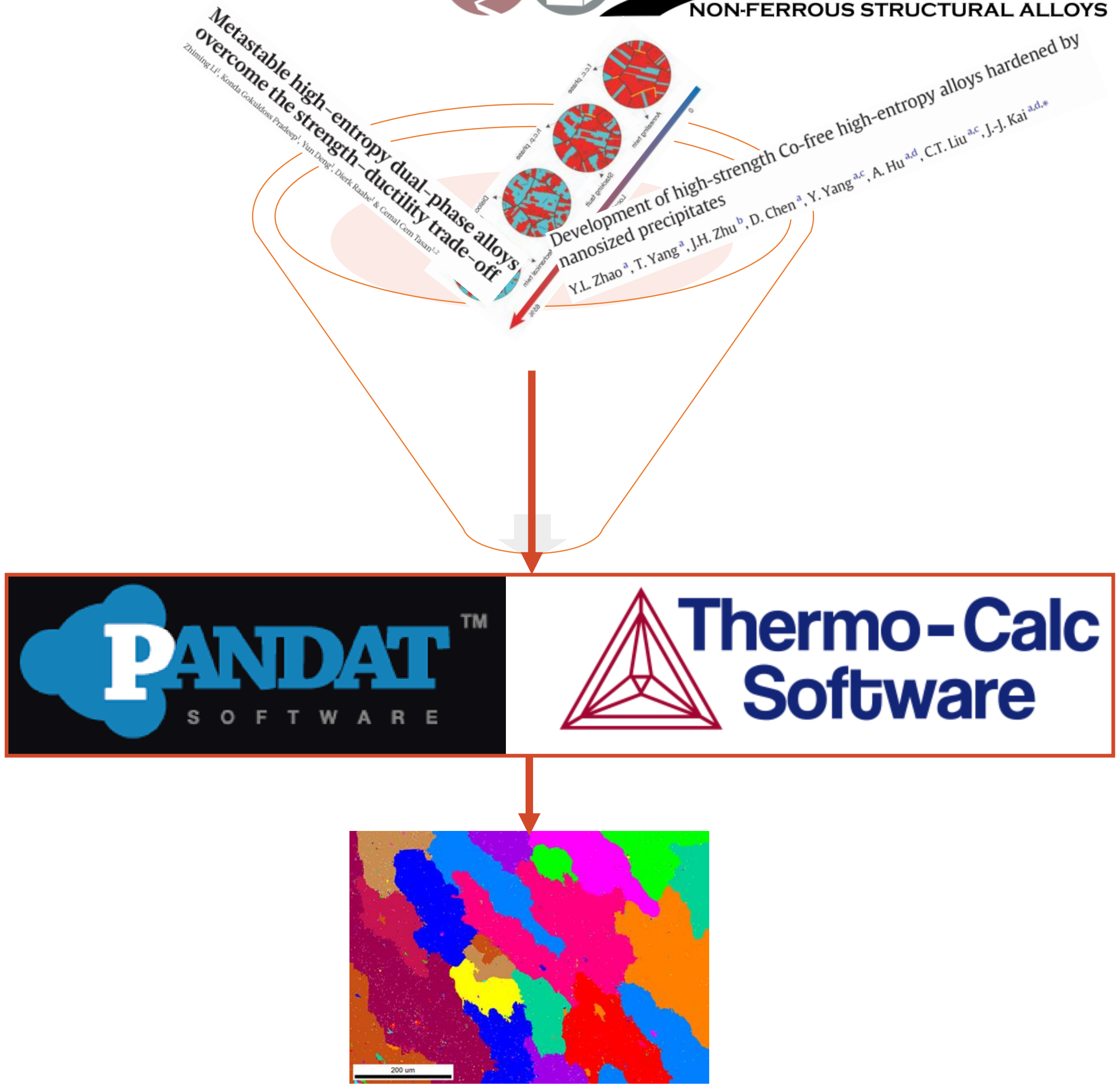

Industry Sponsor Baseline Alloys - ATI

CANFSA
CENTER FOR ADVANCED NON-FERROUS STRUCTURAL ALLOYS

- Three alloys from industry sponsor ATI
- Processing & mechanical behavior references for specific property/chemistry spaces
- ATI 188 – Co-base high-temp austenitic alloy; high work-hardening; TRIP?
- A286 – Legacy NiCr high-temp austenitic steel; γ' precipitate strength; TRIP?
- Datalloy HP – Highly alloyed steel; quasi-MPEA

ATI

Center Proprietary – Terms of CANFSA Membership Agreement Apply

Alloy Design Concepts

Basic factors:

- Metastability (TRIP)
- Deformation twinning (TWIP)
- Solid solution strengthening

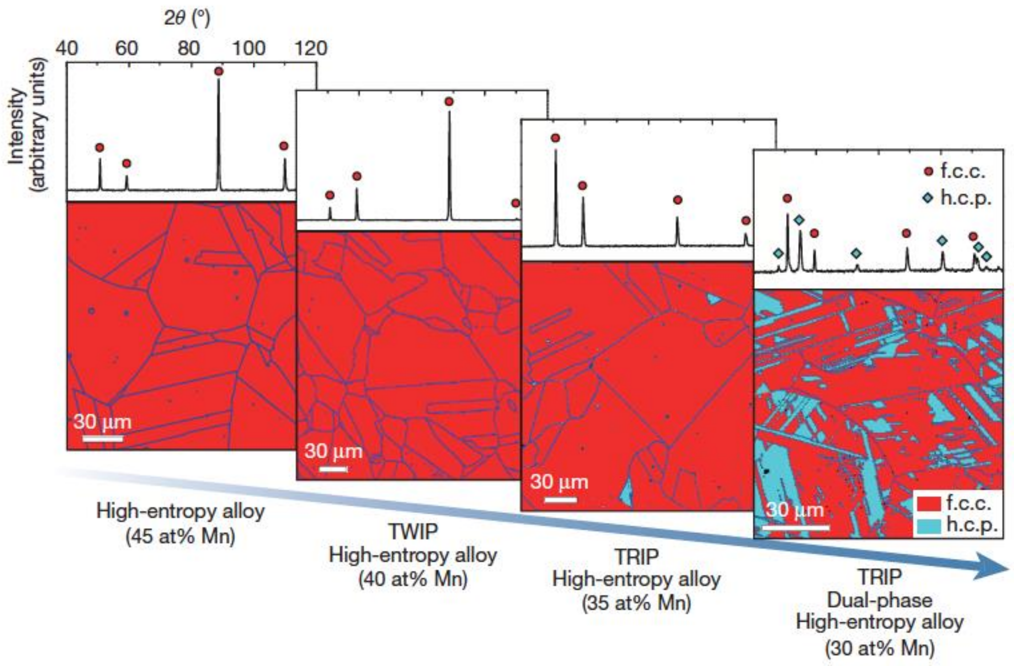

Z. Li et al. *Nature* 2016

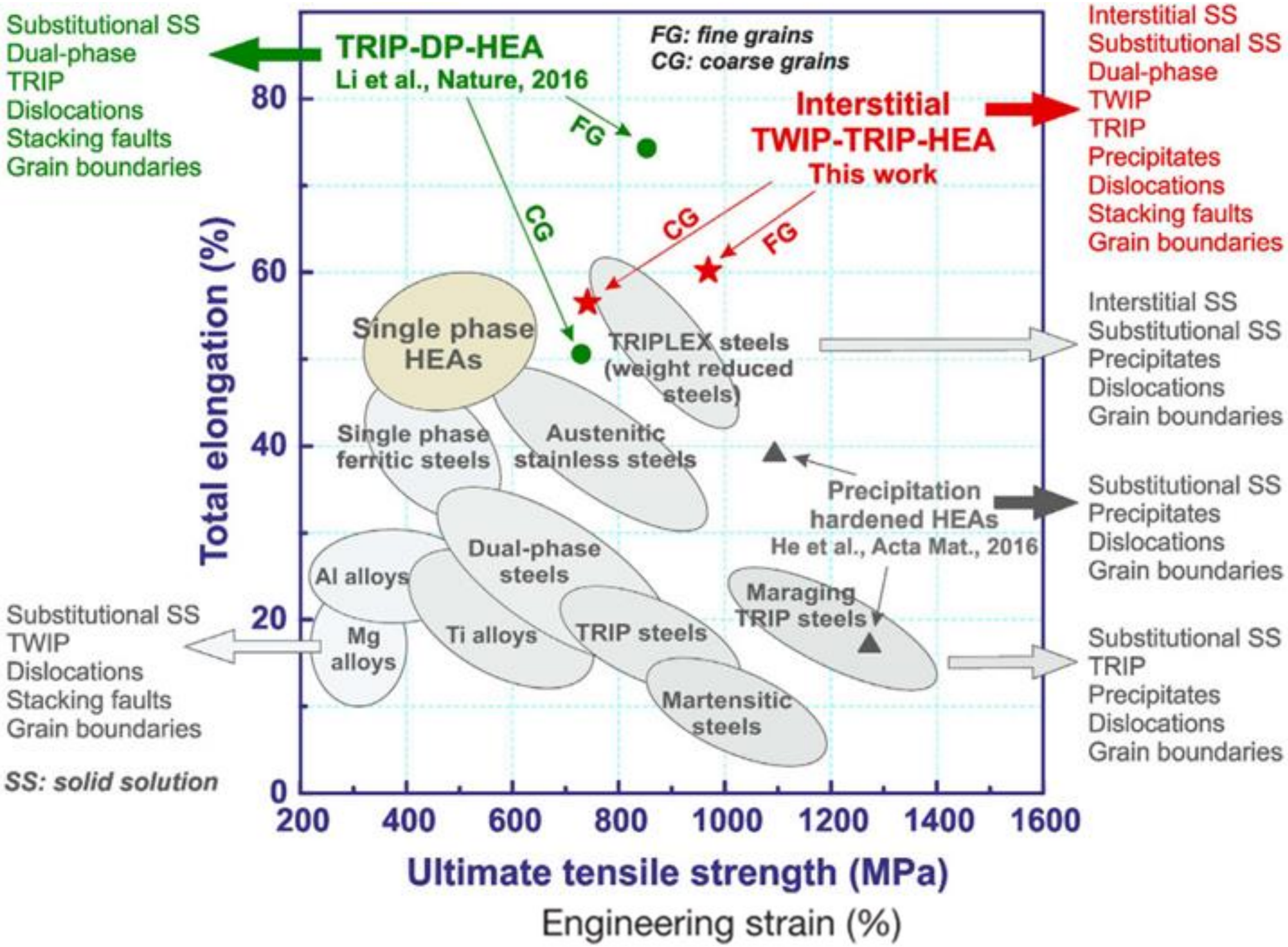

Z. Li et al, *Sci Rep* 2017

Thermodynamic Screening – T_0 & Strain-Induced Martensitic Transformations

CENTER FOR ADVANCED NON-FERROUS STRUCTURAL ALLOYS

Thermo-Calc Software

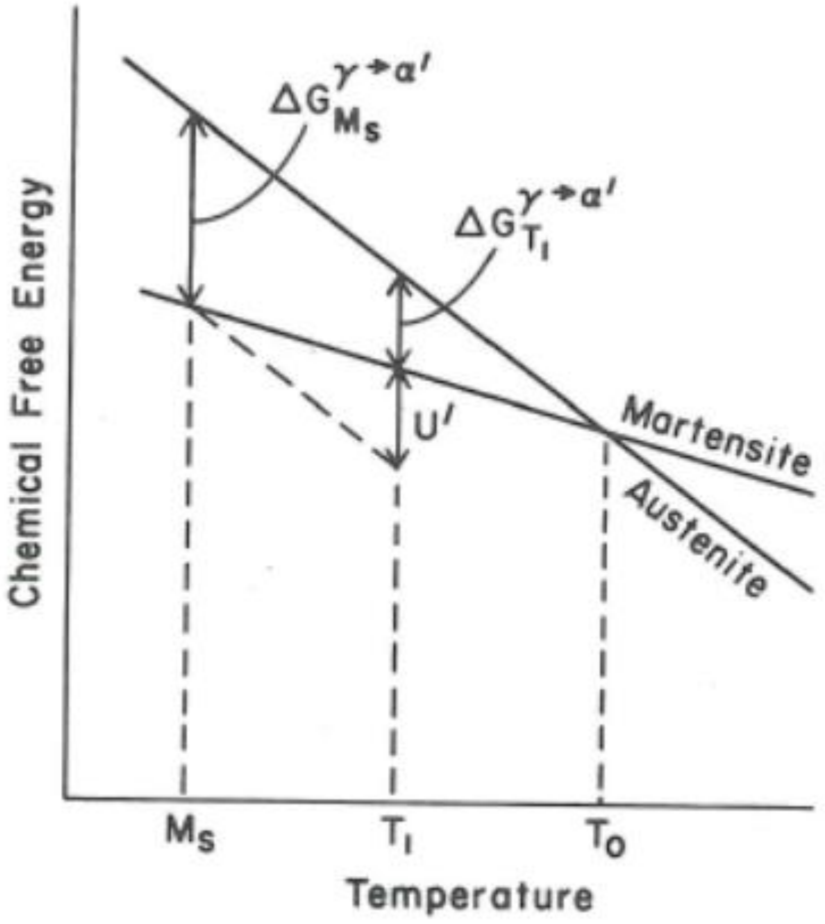

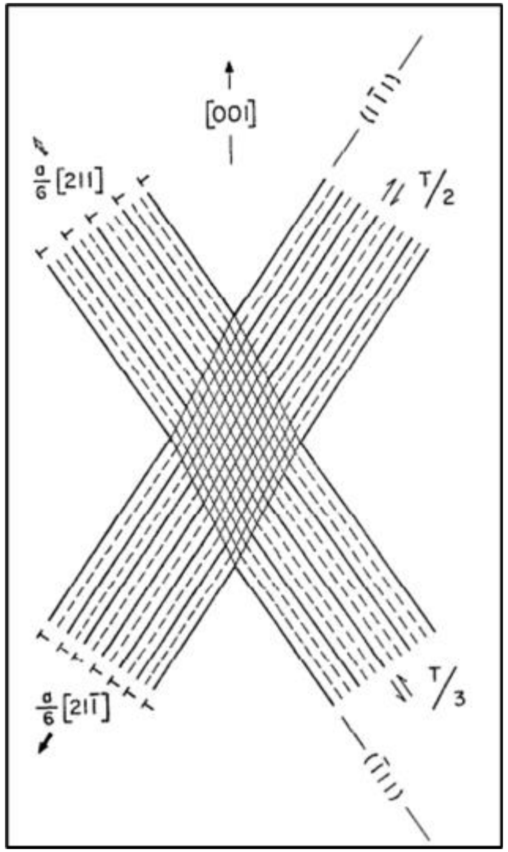

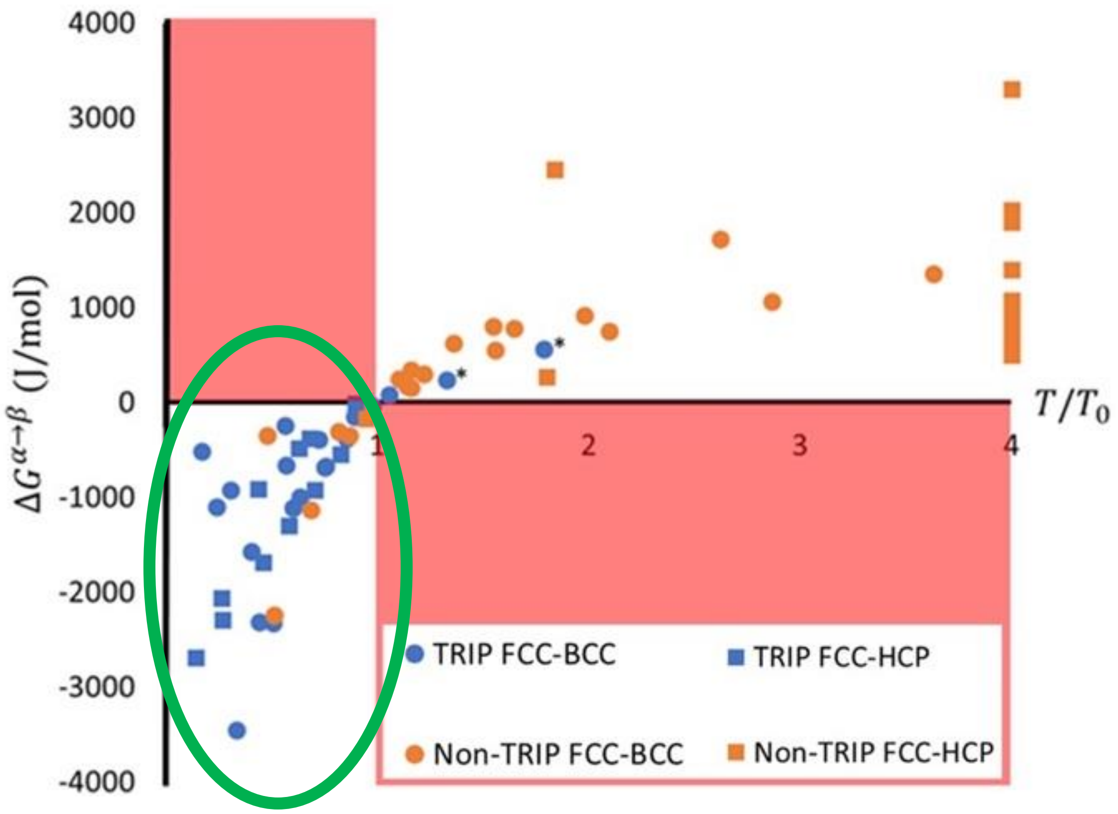

J.A. Copley, MS Thesis, Colorado School of Mines, 2020

Martensite, Ed. G.B. Olson and W.S. Owen, ASM International, 1992

Thermodynamic Screening – T_0 & Strain-Induced Martensitic Transformations

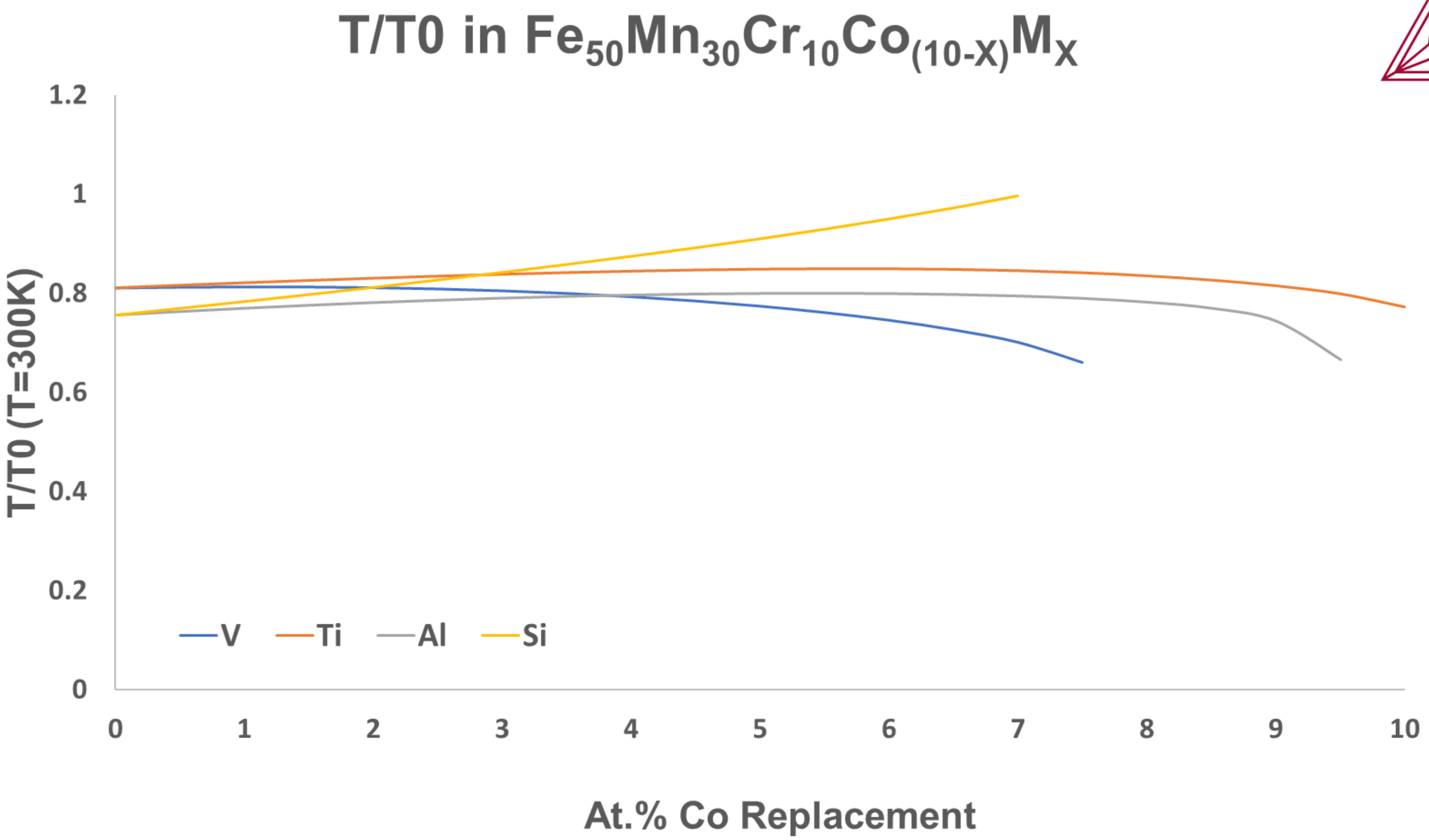

Solid Solution Strength Modeling in MPEAs

- MPEAs considered to have high SSH – significant size, modulus misfit effects
- Modified Toda-Caraballo (2015) model using “effective atomic radii” (Coury 2018)
- “TC-EARS” model has best-in-class predictivity of MPEA SSH
- Easily implemented in Python using phase comp inputs from Thermocalc

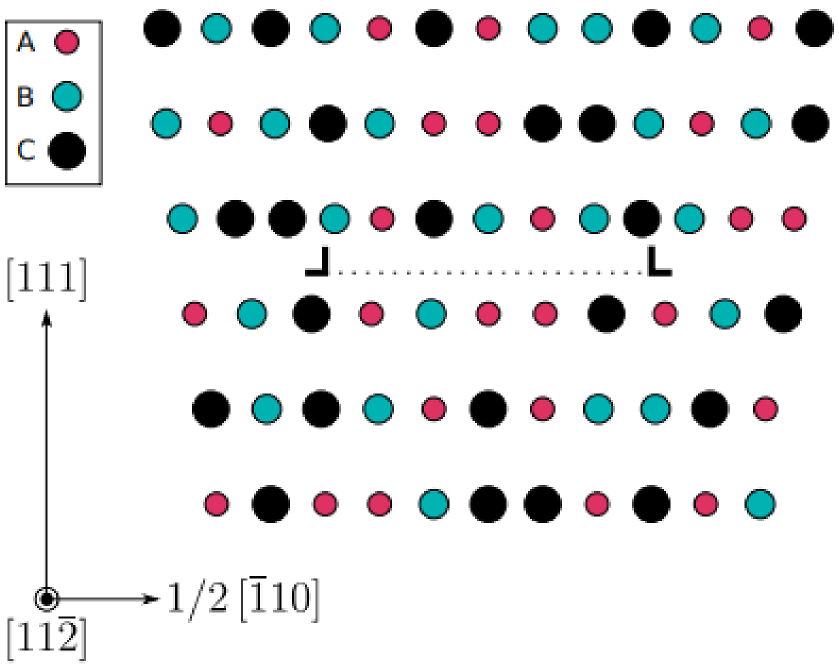

Varvenne, Luque & Curtin, *Acta Mater* 2016

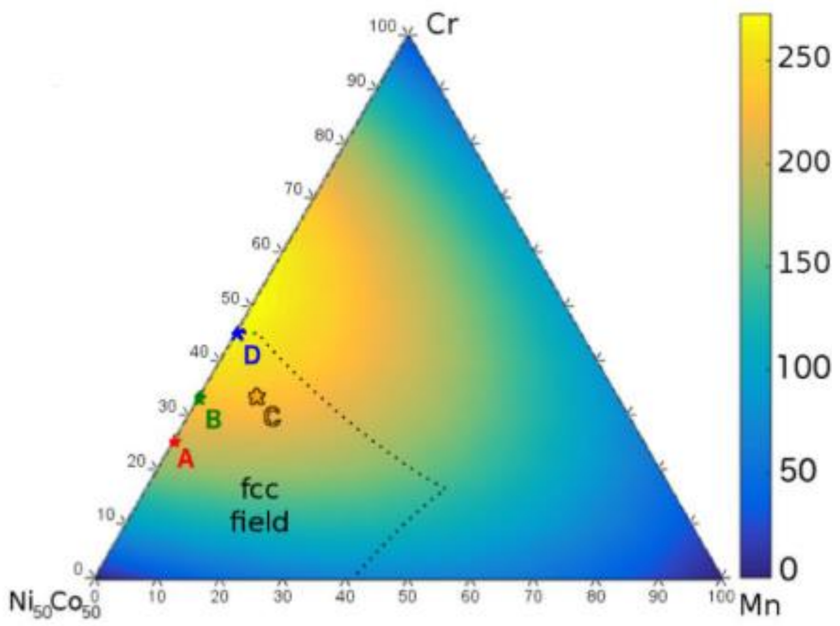

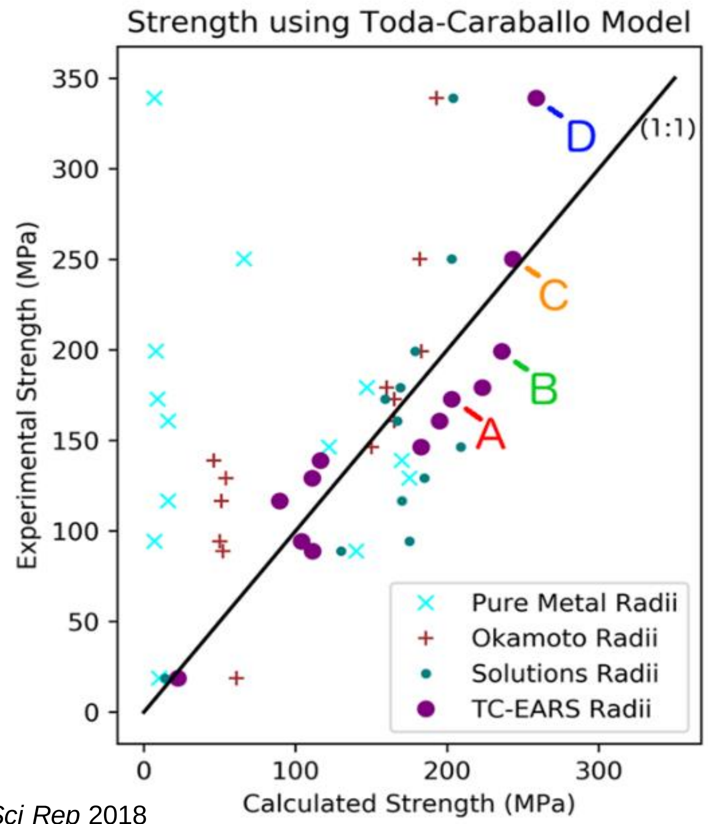

Coury et al, *Sci Rep* 2018

Multifactor Screening – Metastability With Solid Solution Strengthening

CANFSA
CENTER FOR ADVANCED NON-FERROUS STRUCTURAL ALLOYS
Thermo-Calc Software

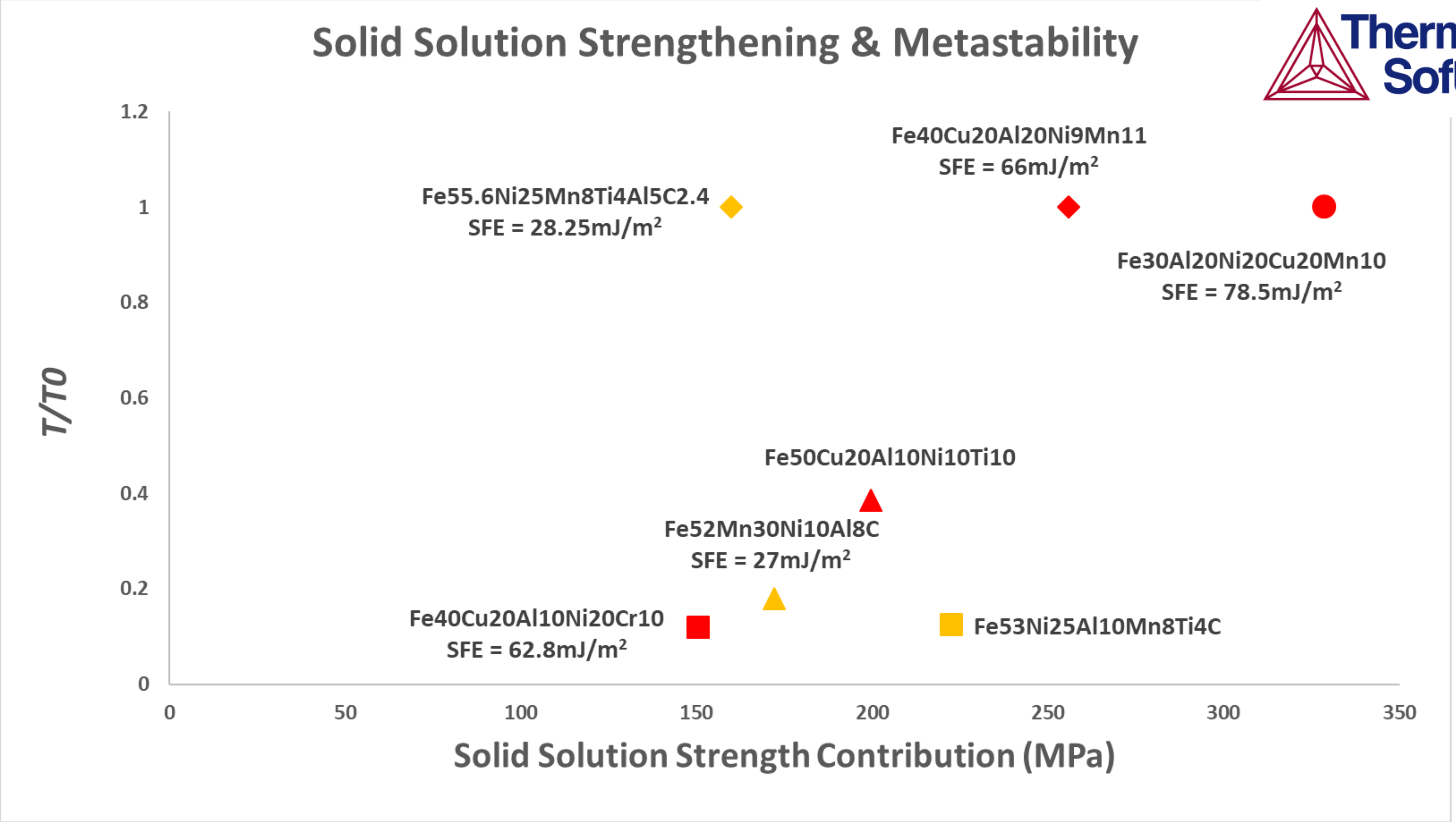

Alloy Design Concepts

Basic factors:

- Metastability (TRIP)
- Deformation twinning (TWIP)
- Solid solution strengthening

Microstructural features:

- Limit brittle IMs (σ, μ, χ phases)
- γ' precipitate strengthening
- Other precipitates (carbides, Fe_2SiTi)
- GB pinning – precipitates, Nb
- Overaged precipitates (reduce ASB)

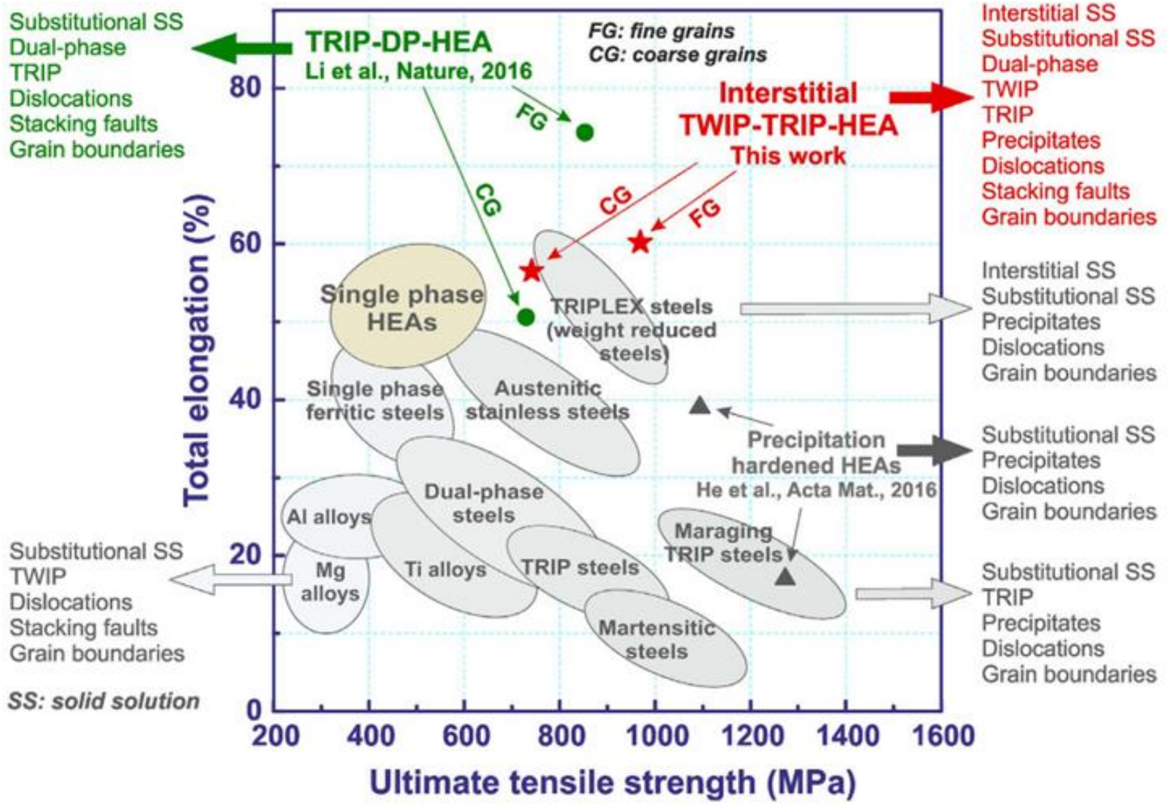

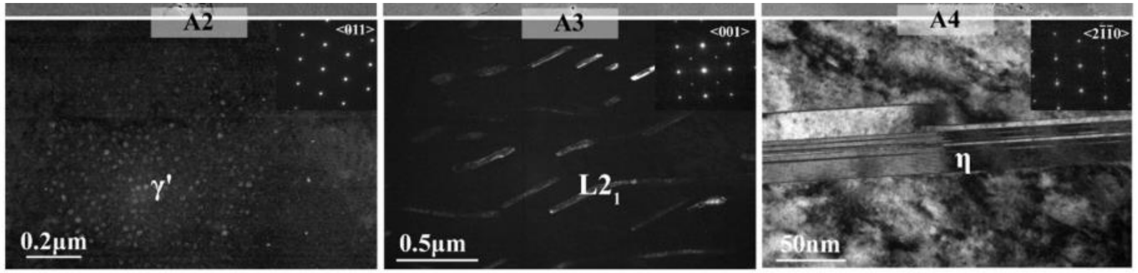

Ti/Al=0.6 Ti/Al=1 Ti/Al=1.7

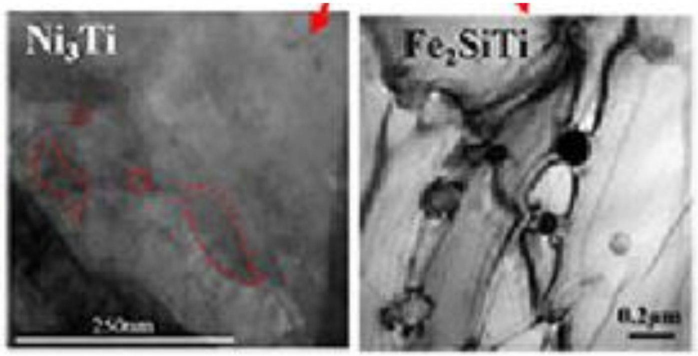

Top: Z. Li et al, *Sci Rep* 2017

Left: F. Haftlang et al, *Scripta Mater* 2021

Far left:

Literature Guided Design for Precipitation – Fe_2SiTi

$Fe_{65}Ni_{15}Co_8Mn_8Ti_3Si$–Haftlang et al. 2021

- TRIP/TWIP active with fine precipitates
- >1GPa YS, higher WHR than $Fe_{50}Mn_{30}Co_{10}Cr_{10}$
- Can we remove Co?

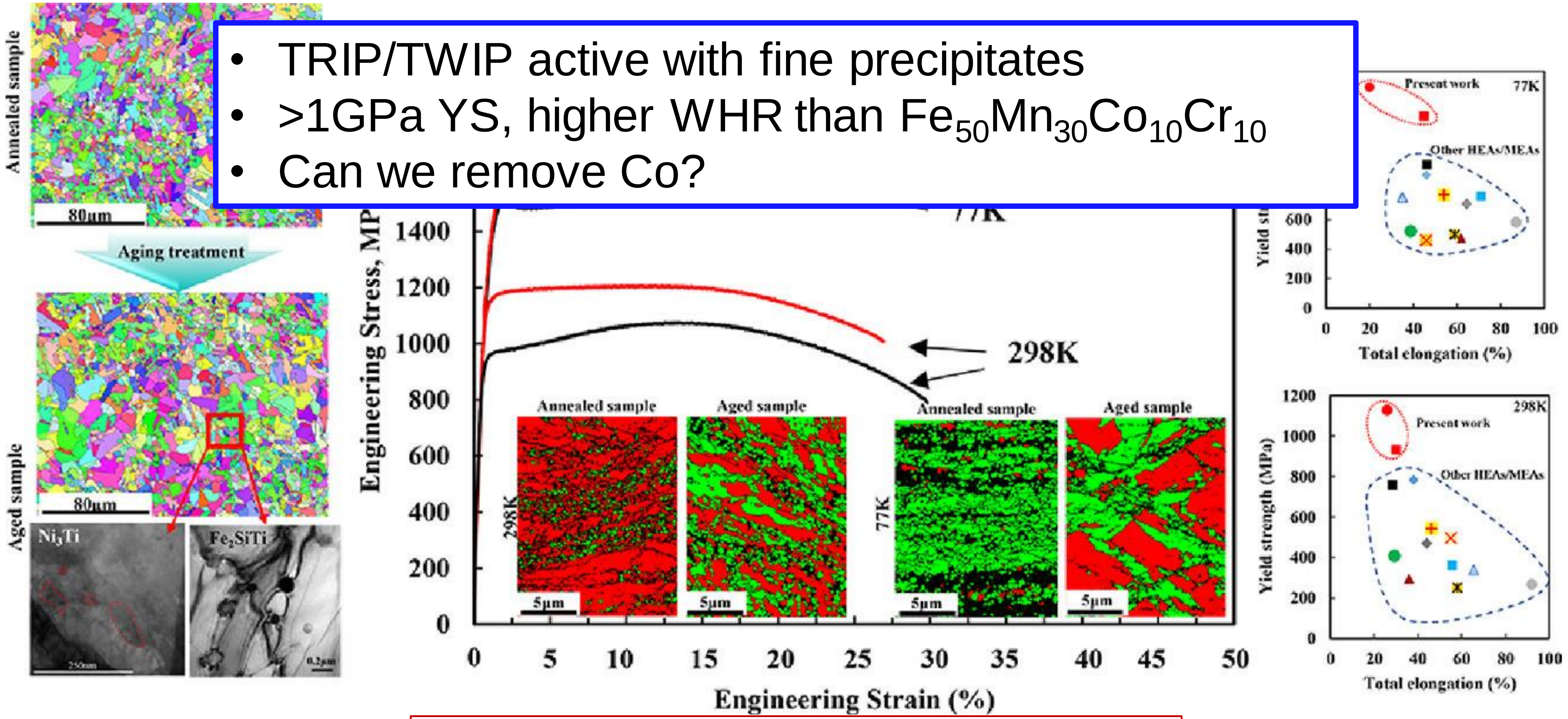

Literature Guided Design for Precipitation – Fe_2SiTi

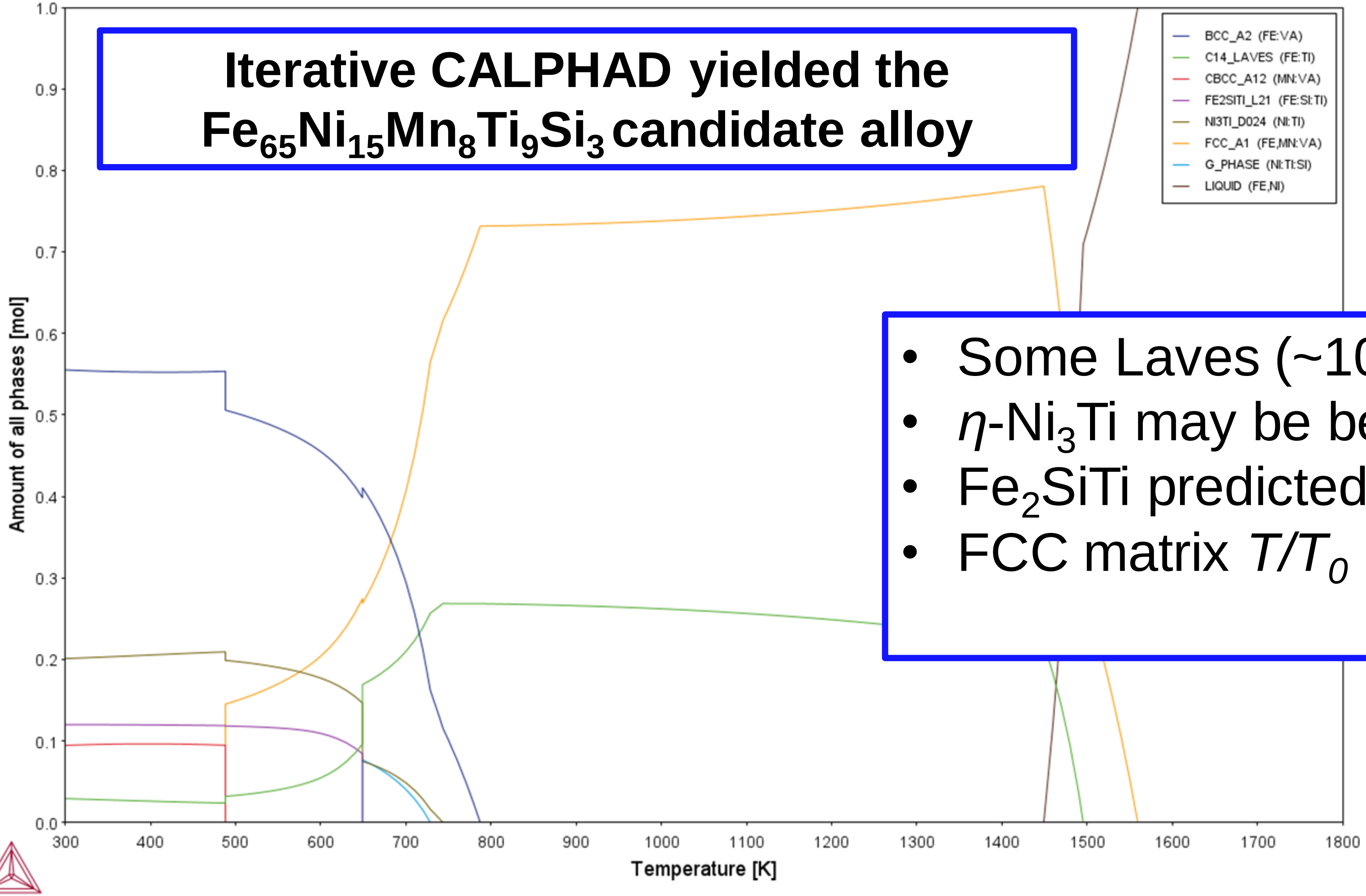

- Some Laves (~10% <350°C)
- η-Ni_3Ti may be beneficial
- Fe_2SiTi predicted (12%)
- FCC matrix T/T_0 = 0.49 predicted

Literature Guided Design for Precipitation – γ’/$L1_2$

- γ’ strengthened TRIP assisted armor

Composition	Max γ’ %	Sigma phase	Other Precipitates
$Fe_{58}Ni_{25}Al_{10}Mn_8Ti_4C_{2.4}$	15% - 330°C	None	η-Ni_3Ti (5%)
$Fe_{45}Ni_{28}Cr_8Mn_8Al_5Ti_6Nb_{.25}$	28% - 225°C	Present @ all γ’ T, ~20%	η-Ni_3Ti (26% @ 500°C)
$(FeNi)_{67}Cr_{15}Mn_{10}Al_3Ti_5Nb_{.25}$	32% - 350°C	Present @ all γ’ T, ~35%	η-Ni_3Ti (26% @ 550°C)

Caveat to precipitation modeling in MPEAs: require experiment for accurate growth model inputs – This is a goal for Year 2 of this project

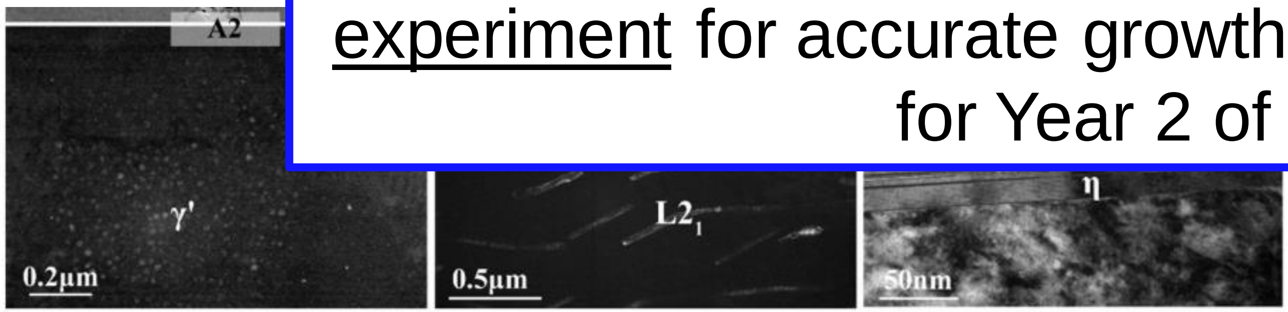

Ti/Al=0.6 Ti/Al=1 Ti/Al=1.7

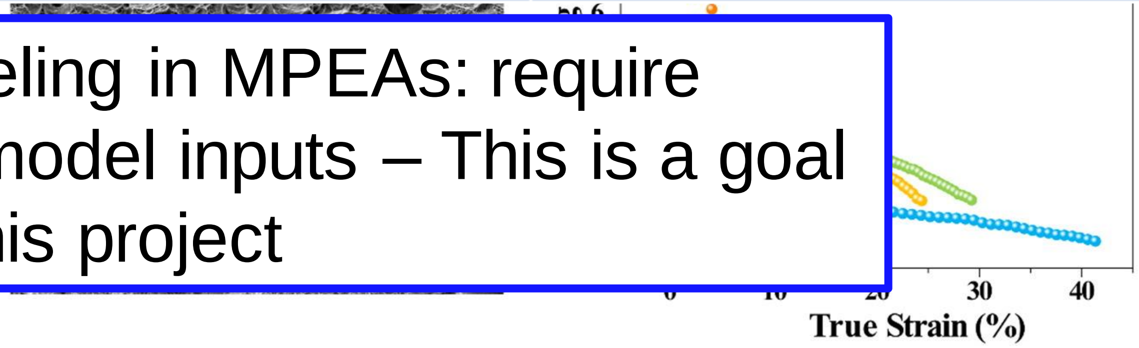

$(FeNi)_{67}Cr_{15}Mn_{10}Al_{8-x}Ti_x$ (x=3-5 at.%)

Alloy Design Progress

CANFSA
CENTER FOR ADVANCED NON-FERROUS STRUCTURAL ALLOYS

Goal: 6 experimental alloys
(3-4 SS TRIP/TWIP, 2-3 precipitate strengthened)
Result: >10 candidates identified – Risk Mitigation

Decision metrics:

1. Solid solution strength vs. T/T_0, calculated SFE
2. Precipitate fraction vs. T/T_0, SFE
3. SSS vs. precipitate fraction
4. Presence & calculated kinetics of brittle IMs

SS TRIP/TWIP	γ' $Ni_3(Al,Ti)$	Other precip/IM
1. $Fe_{58}Mn_{25}Ni_{10}V_7$ 2. $Fe_{60}Ni_{30}V_{10}$ 3. $Fe_{40}Cu_{20}Ni_{20}Al_{10}Cr_{10}$ 4. Nb microalloyed $Fe_{50}Mn_{30}Co_{10}Cr_{10}$	1. $Fe_{55.6}Ni_{25}Mn_8Al_5Ti_4C_{2.4}$ 2. $Fe_{46}Ni_{28}Cr_7Mn_8Al_5Ti_4Nb$ 3. $(FeNi)_{67}Cr_{15}Mn_{10}Al_3Ti_5Nb$	1. $Fe_{65}Ni_{15}Mn_8Ti_8Si_3$ 2. $Fe_{55}Mn_{25}Al_{10}Si_7Mo_3$ 3. $Fe_{50}Mn_{26}Ni_{14}Si_6Mo_4$

All compositions given in at.%

Alloy Design Progress

CANFSA
CENTER FOR ADVANCED NON-FERROUS STRUCTURAL ALLOYS

Goal: 6 experimental alloys
(3-4 SS TRIP/TWIP, 2-3 precipitate strengthened)
Result: >10 candidates identified – Risk Mitigation

Decision metrics:

1. **Solid solution strength vs. T/T_0, calculated SFE**
2. **Precipitate fraction vs. T/T_0, SFE**
3. **SSS vs. precipitate fraction**
4. **Presence & calculated kinetics of brittle IMs**

SS TRIP/TWIP	γ' $Ni_3(Al,Ti)$	Other precip/IM
1. $Fe_{58}Mn_{25}Ni_{10}V_7$	1. $Fe_{55.6}Ni_{25}Mn_8Al_5Ti_4C_{2.4}$	1. $Fe_{65}Ni_{15}Mn_8Ti_8Si_3$
2. $Fe_{60}Ni_{30}V_{10}$	2. $Fe_{46}Ni_{28}Cr_7Mn_8Al_5Ti_4Nb$	2. $Fe_{55}Mn_{25}Al_{10}Si_7Mo_3$
3. $Fe_{40}Cu_{20}Ni_{20}Al_{10}Cr_{10}$	3. $(FeNi)_{67}Cr_{15}Mn_{10}Al_3Ti_5Nb$	3. $Fe_{50}Mn_{26}Ni_{14}Si_6Mo_4$
4. Nb microalloyed $Fe_{50}Mn_{30}Co_{10}Cr_{10}$		

All compositions given in at.%

Candidate MPEA #1 - $Fe_{55.6}Ni_{25}Mn_8Al_5Ti_4C_{2.4}$

- $Fe_{55.6}Ni_{25}Mn_8Al_5Ti_4C_{2.4}$ – σ-free γ'-strengthened FCC MPEA with predicted matrix metastability
- Age hardening with higher peak age hardness than ATI A286 reference alloy
- Ductility – cold rolled >50% with no cracking

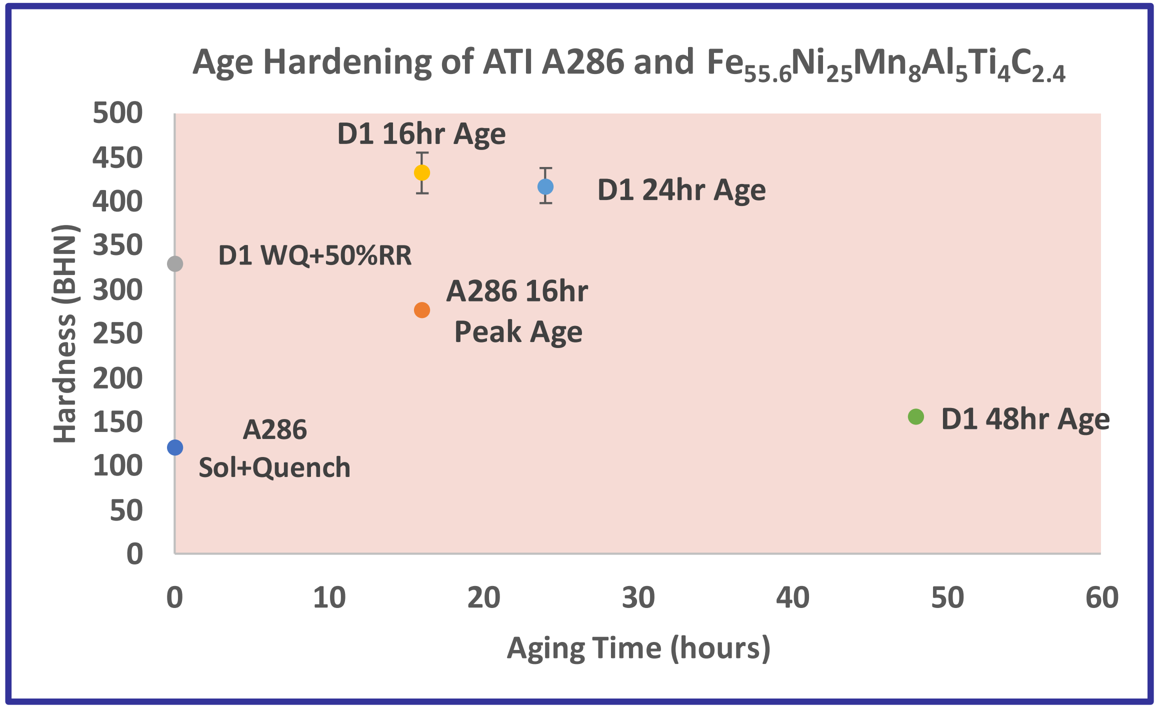

$Fe_{55.6}Ni_{25}Mn_8Al_5Ti_4C_{2.4}$ Characterization

- **48hr age, 540°C**

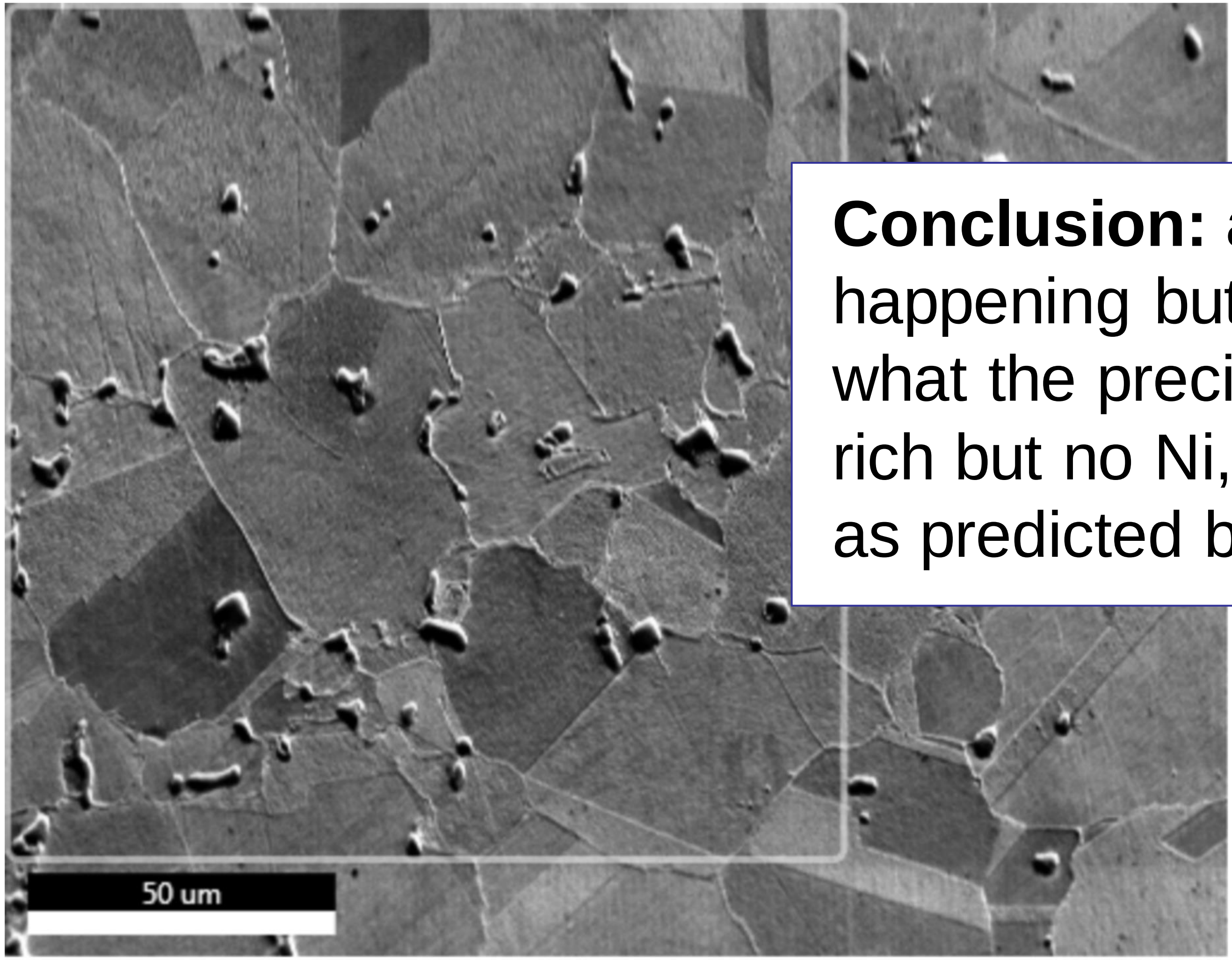

Conclusion: age hardening is happening but do not yet know what the precipitates are; Ti-rich but no Ni, Al = not γ’ or η as predicted by Thermo-Calc

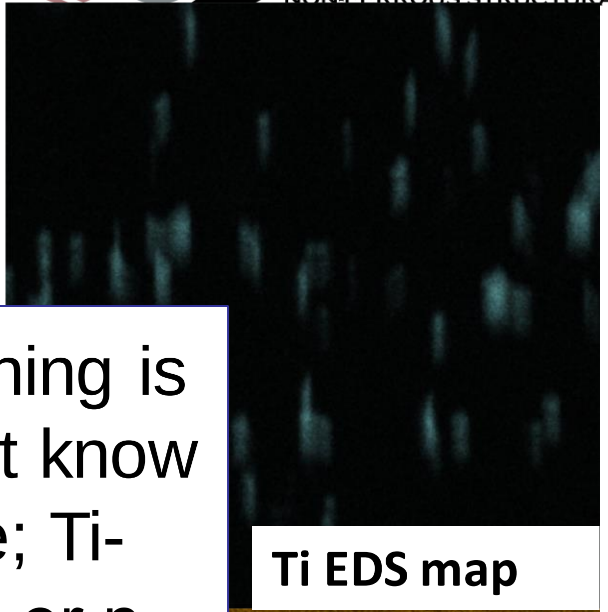

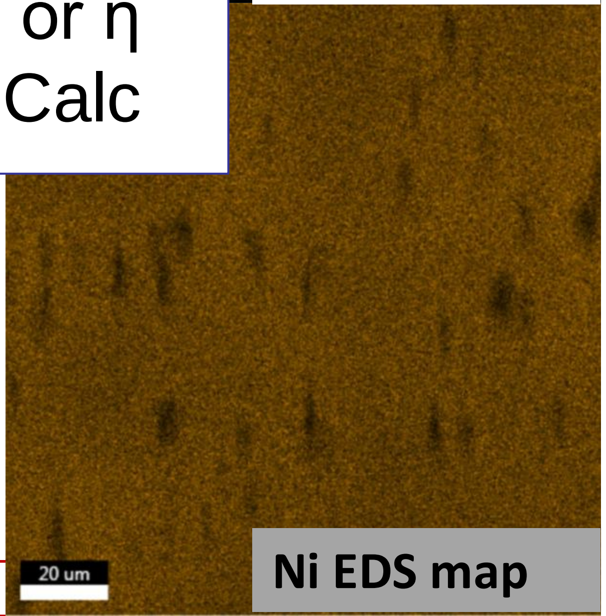

ATI Baseline Alloys Status

- Heat treatment, sample prep & etchant procedures identified for Datalloy HP

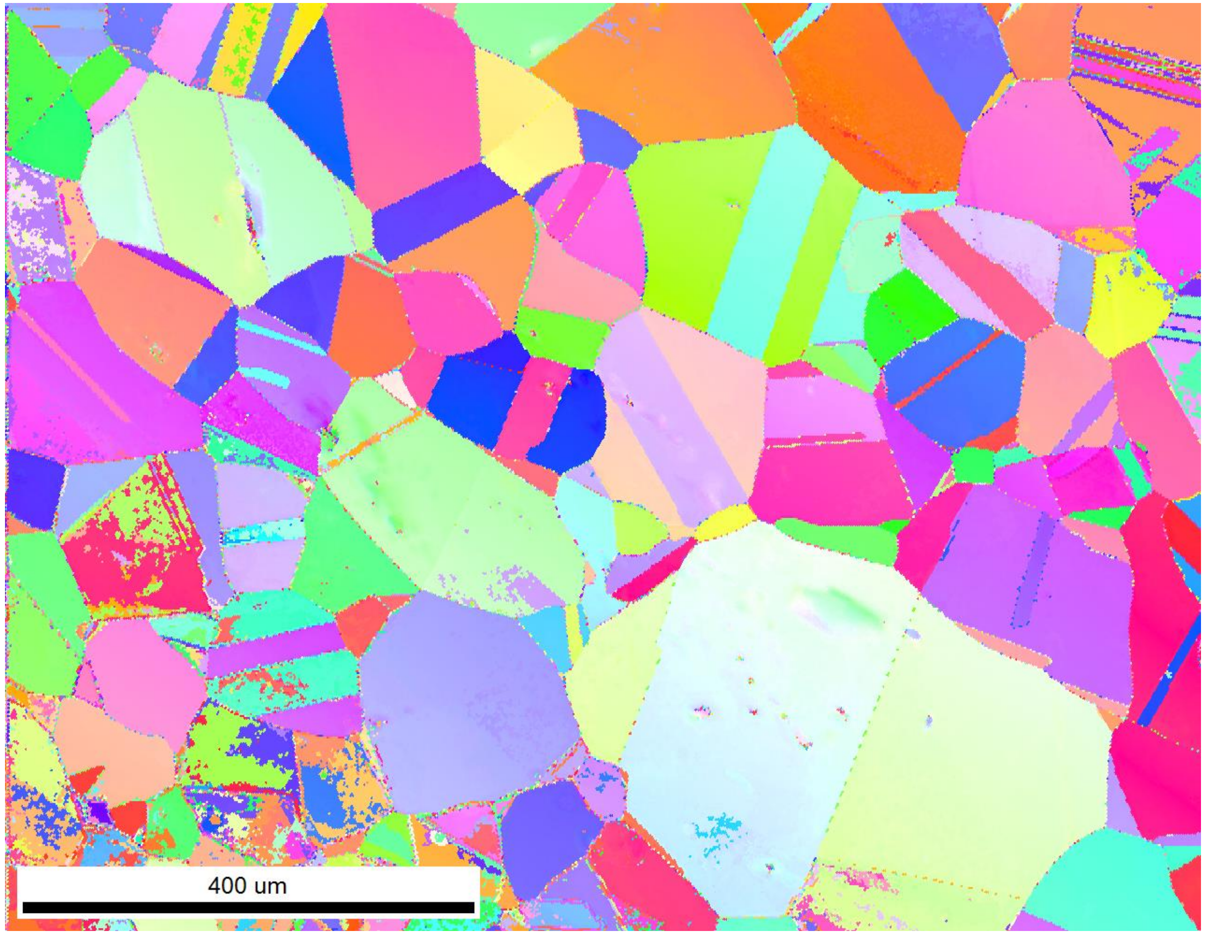

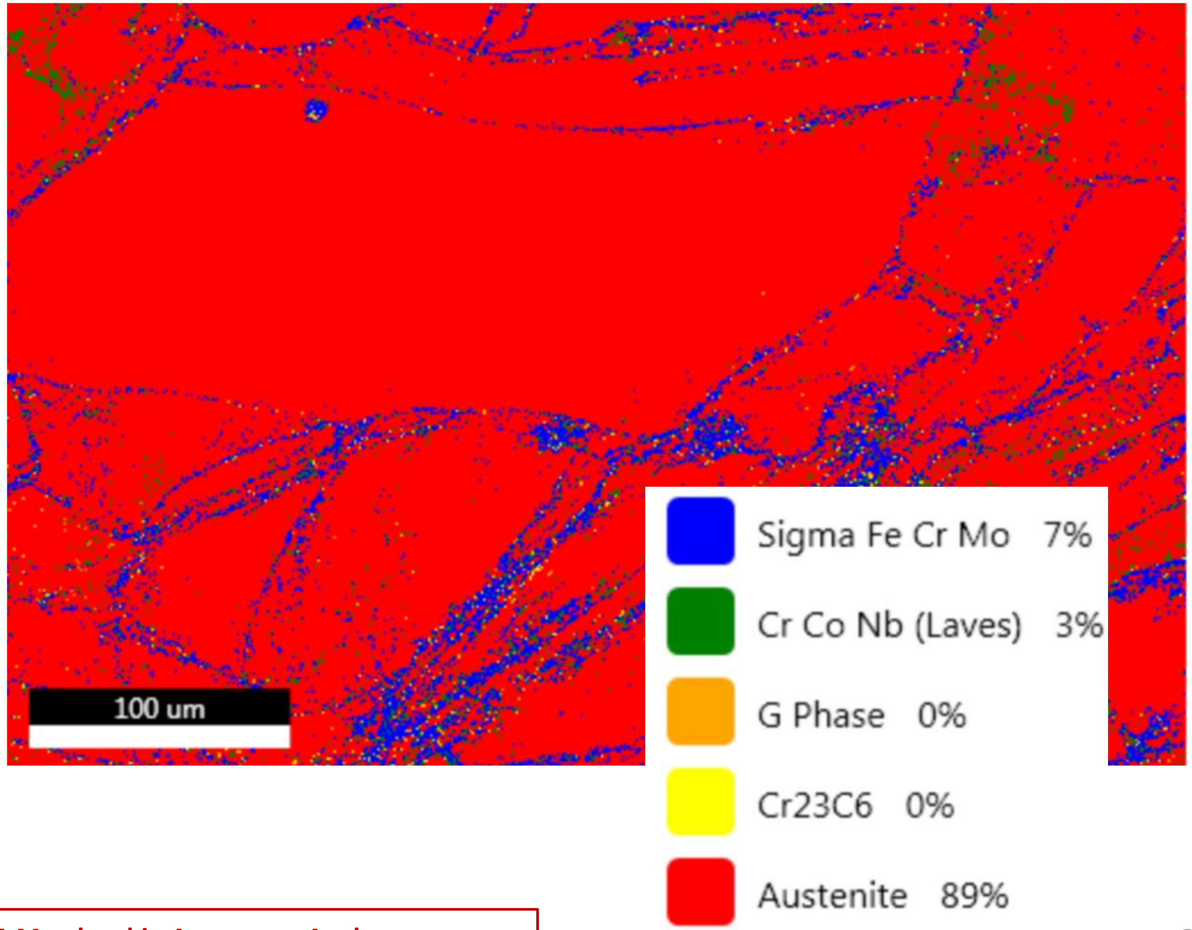

Arc Melt Furnace Status

CANFSA
CENTER FOR ADVANCED NON-FERROUS STRUCTURAL ALLOYS

- Installed & commissioned December 2021
- Currently functional and producing samples – project risk reduction
- Chemistry analysis samples sent to 3rd party lab to assess O, N pickup, Mn fade
- In process of buying add’l molds e.g plate

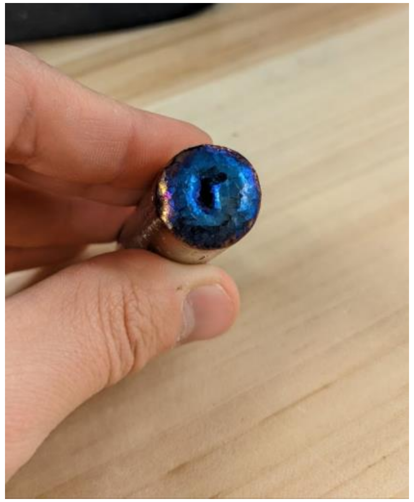

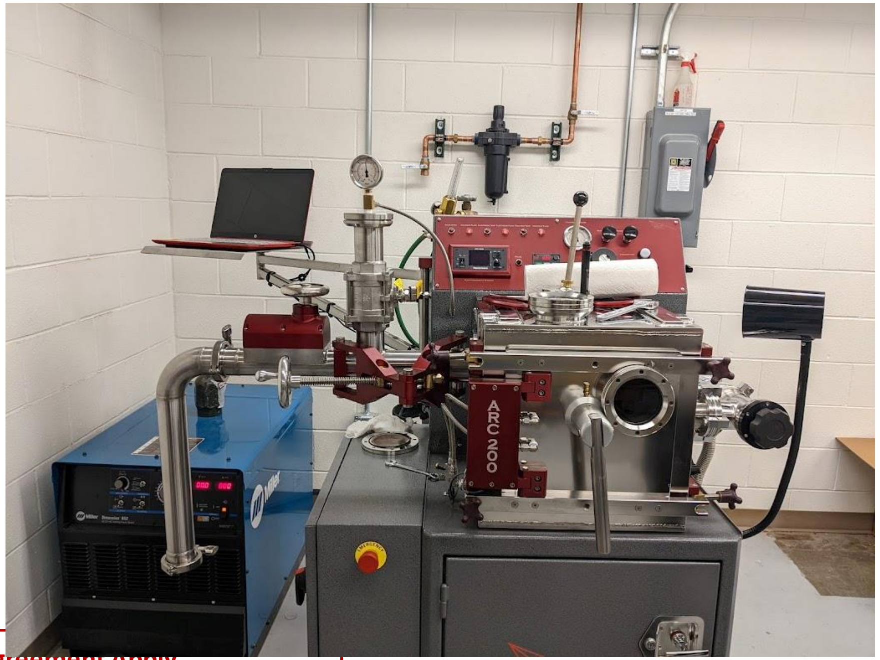

Year 2 Roadmap

- Arc melter production of candidate alloys (slide 9)
- Produce & characterize desired microstructures
- Mechanical testing – multiple T, strain rates
- Assess failed samples to understand microstructure – deformation mechanism – performance links

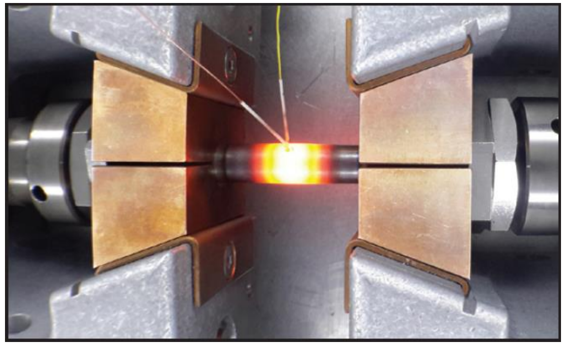

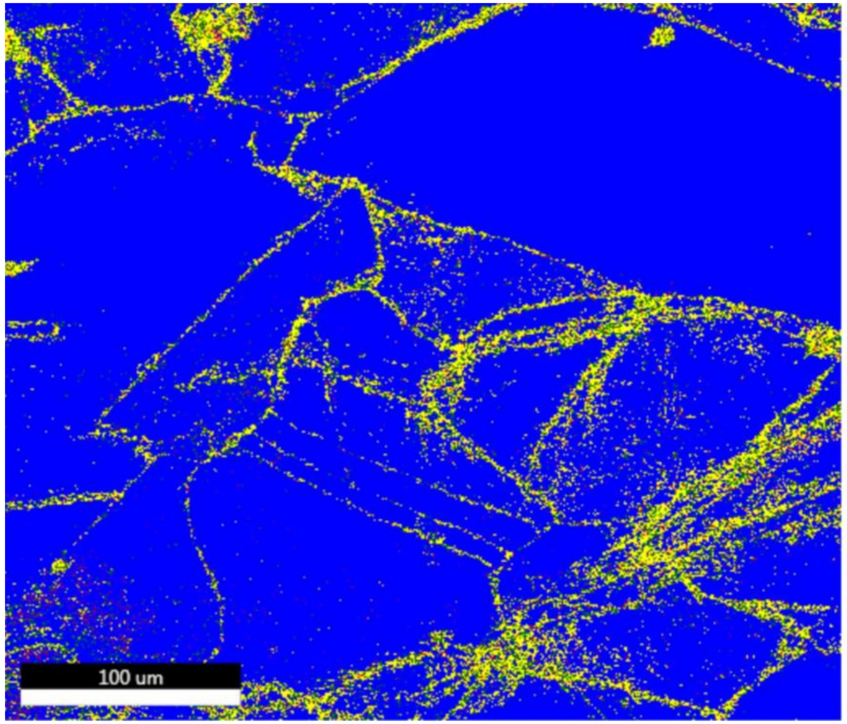

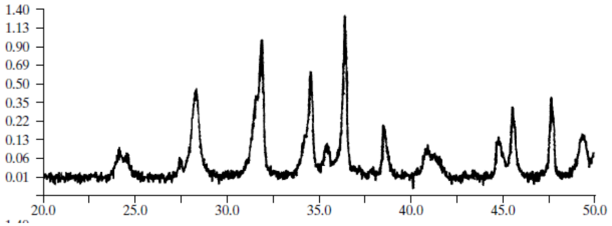

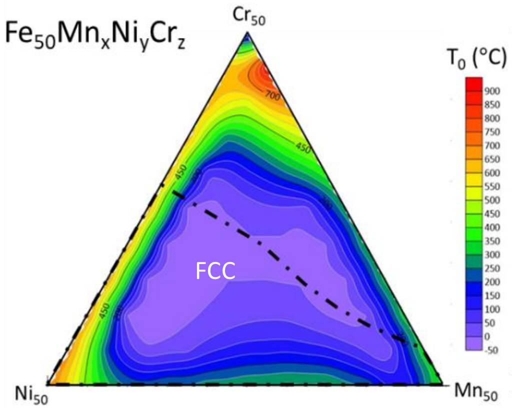

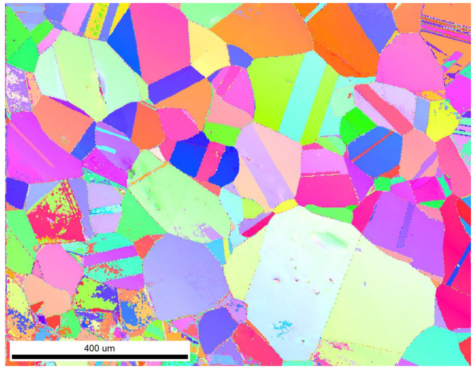

Gantt Chart

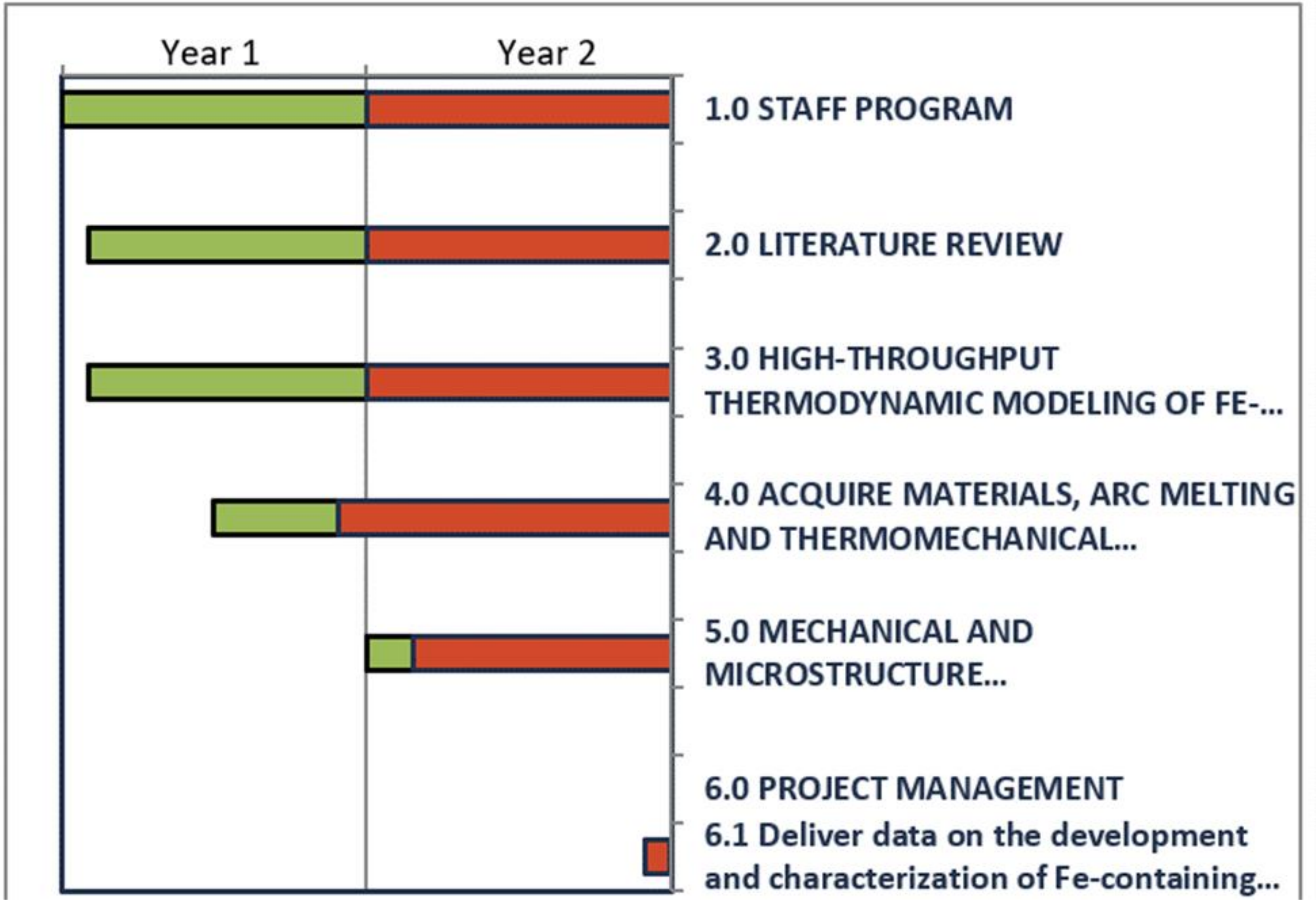

Year 1
Year 2
1.0 STAFF PROGRAM
2.0 LITERATURE REVIEW
3.0 HIGH-THROUGHPUT THERMODYNAMIC MODELING OF FE-...
4.0 ACQUIRE MATERIALS, ARC MELTING AND THERMOMECHANICAL...
5.0 MECHANICAL AND MICROSTRUCTURE...
6.0 PROJECT MANAGEMENT
6.1 Deliver data on the development and characterization of Fe-containing...

Acknowledgements

- This program is sponsored by the Defense Logistics Agency – Troop Support, Philadelphia PA and the Defense Logistics Agency Information Operations, J68, Research & Development, Ft. Belvoir, VA.
- Special thanks is also given to ATI Specialty Materials for providing test materials.
- Particular thanks also go to Dr. Krista Limmer at DEVCOM Army Research Laboratory.

References

1. I. Crouch, *The Science of Armour Materials,* Elsevier (2017)
2. A. Doig, *Military Metallurgy*, Maney Publishing: London (1998)
3. D.K. Matlock and J.G. Speer, “Design considerations for the next generation of advanced high strength steels”, *Proceedings of The 3rd International Conference on Advanced Structural Steels*, Gyeongju, Korea, 2006, pp. 774-781
4. Y.F. Ye, Q. Wang, J. Lu, C.T. Liu, Y. Yang. “High-entropy alloy: challenges and prospects”, *Materials Today*, 2011, 19(6):349-362
5. Z. Li, C.C. Tasan, H. Springer, B. Gault, D. Raabe, “Interstitial atoms enable joint twinning and transformation induced plasticity in strong and ductile high-entropy alloys”, *Scientific Reports*, 2017, 7:40704
6. G.Bertoli, L. Otani, A.J. Clarke, C. S. Kiminami, F.G. Coury, “Hall–Petch and grain growth kinetics of the low stacking fault energy TRIP Cr40Co40Ni20 multi-principal element alloy”, *Applied Physics Letters* 119, 061903 (2021)
7. Z. Li, K.G. Pradeep, Y. Deng, D. Raabe, C.C. Tasan, “Metastable high-entropy dual-phase alloys overcome the strength-ductility trade-off”, *Nature*, 2016, 534:227-230
8. J.A. Copley, Prediction and Observation of Transformation-Induced Plasticity Behavior in CoCrNi Multi-Principal Element Alloys with In-Situ Synchrotron X-Ray Diffraction, MS Thesis, Colorado School of Mines, 2020
9. C. Varvenne, A. Luque, W.A. Curtin, Theory of strengthening in fcc high entropy alloys, *Acta Materialia* 118 (2016) 164–176.
10. I. Toda-Caraballo, P.E.J. Rivera, R.D del Castillo, Modelling solid solution hardening in high entropy alloys, *Acta Materialia* 85 (2015) 14-23.
11. F.G. Coury, K.D. Clarke, C.S. Kiminami, M.J. Kaufman, A.J. Clarke, High Throughput Discovery and Design of Strong Multicomponent Metallic Solid Solutions, *Scientific Reports* 8 (2018) 1–10.

References

12. F. Haftlang, P. Asghari-Rad, J. Moon, A. Zargaran, K.A. Lee, S.J. Hong, H.S. Kim, "Simultaneous effects of deformation-induced plasticity and precipitation hardening in metastable non-equiatomic FeNiCoMnTiSi ferrous medium-entropy alloy at room and liquid nitrogen temperatures", *Scripta Materialia* 2021 114013
13. Y.L. Zhao, T. Yang, J.H. Zhu, D. Chen, Y. Yang, A. Hu, C.T. Liu, J.J. Kai, "Development of high-strength Co-free high-entropy alloys hardened by nanosized precipitates," *Scripta Materialia* 148 (2018) 51–55.

Supplementary Slides

Industry Sponsor Baseline Alloys - ATI

CANFSA
CENTER FOR ADVANCED NON-FERROUS STRUCTURAL ALLOYS

ATI 188

Limiting Chemical Composition of ATI 188™ Alloy (AMS 5608 Specification Limits for UNS R30188)	
Element	**Weight Percent**
Carbon	0.05 – 0.15
Manganese	1.25 max
Silicon	0.20 – 0.50
Phosphorus	0.020 max
Sulfur	0.015 max
Chromium	20.00 - 24.00
Nickel	20.00 - 24.00
Tungsten	13.00 – 16.00
Lanthanum	0.02 – 0.12
Boron	0.015 max
Iron	3.00 max
Cobalt	Remainder

Datalloy HP

Composition Range (UNS N08830)			
Element	**Wt. %**	**Element**	**Wt. %**
Carbon	0.015	Manganese	3.0 – 6.0
Phosphorous	0.035	Sulfur	0.010
Silicon	1.00	Nickel	29.0 – 34.0
Chromium	20.0 – 24.0	Molybdenum	4.5 – 6.5
Copper	0.50 – 2.00	Cobalt	0.50 – 3.50
Tungsten	0.20 – 1.80	Nitrogen	0.20 – 0.55
Iron	balance		
Maximum % unless a range is indicated.			

A286

Chemical Composition of ATI A286™ Alloy													
	C	Mn	Si	S	P	Cr	Ni	Fe	Mo	Ti	Al	B	V
wt. %, min.	-	1.0	-	-	-	13.5	24.0	Bal.	1.0	1.90	-	0.003	0.10
wt. %, max.	0.08	2.0	1.0	0.015	0.025	16.0	27.0	-	1.5	2.35	0.35	0.010	0.50

30

Industry Partner – ATI Specialty Materials

Added Capability

- 25 & 50 lb. vacuum melted ingots
- VAR/ESR for cleanliness
- Industrial thermomechanical processing & heat treatment

Baseline Alloys

- ATI 188 – Co-base high-temp austenitic alloy; high work-hardening; TRIP?
- A286 – Legacy NiCr high-temp austenitic steel; TRIP?
- Datalloy HP – Highly alloyed steel; quasi-MPEA

Composition Range (UNS N08830)			
Element	**Wt. %**	**Element**	**Wt. %**
Carbon	0.015	Manganese	3.0 – 6.0
Phosphorous	0.035	Sulfur	0.010
Silicon	1.00	Nickel	29.0 – 34.0
Chromium	20.0 – 24.0	Molybdenum	4.5 – 6.5
Copper	0.50 – 2.00	Cobalt	0.50 – 3.50
Tungsten	0.20 – 1.80	Nitrogen	0.20 – 0.55
Iron	balance		
Maximum % unless a range is indicated.			

Datalloy HP

$T/T_0 = 0.13$ (FCC→BCC)

Modified Olson-Cohen SFE Algorithm

$$\gamma_{SFE} = 2\rho \ \Delta G^{\gamma\to\varepsilon} + 2\sigma \qquad \rho = \frac{4}{\sqrt{3}}\frac{1}{a^2 N}$$

$$\Delta G^{\gamma\to\varepsilon}_{N(bulk)} = E^{\varepsilon}_N - E^{\gamma}_N \text{ (see Eq. 12)}$$

interstitial nitrogen

$$\Delta G^{\gamma\to\varepsilon} = \sum_i \chi_i \Delta G_i^{\gamma\to\varepsilon} + \sum_{ij} \chi_i \chi_j \Omega_{ij}^{\gamma\to\varepsilon} + \Delta G_{mg}^{\gamma\to\varepsilon} + \Delta G_{seg\,(int)}^{\gamma\to\varepsilon}$$

substitutionals

$$\Delta G_\varphi^{\gamma\to\varepsilon} = (G_\varphi^\varepsilon - G_\varphi^\gamma)$$

$$G_\varphi^\Phi = a + bT + cT\ln(T) + \sum dT^n$$

$$\Omega_{\varphi\phi}^{\gamma\to\varepsilon} = ({}^0L^\varepsilon - {}^0L^\gamma) + ({}^1L^\varepsilon - {}^1L^\gamma)(\chi_\varphi - \chi_\phi)$$

$$\Delta G_{mg}^{\gamma\to\varepsilon} = G_{mg}^\varepsilon - G_{mg}^\gamma$$

$$D = \frac{518}{1125} + \frac{11692}{15975}\left(\frac{1}{p} - 1\right)$$

$$G_{mg}^\Phi = RT\ln(\beta^\Phi + 1) f^\Phi(\tau^\Phi)$$

$$\tau^\Phi = T / T^\Phi_{Néel}$$

$\tau^\Phi \leq 1$

$\tau^\Phi > 1$

$$f^\Phi(\tau^\Phi) = -\left[\frac{\tau^{-5}}{10} + \frac{\tau^{-15}}{315} + \frac{\tau^{-25}}{1500}\right] / D$$

$$f^\Phi(\tau^\Phi) = 1 - \left[\frac{79\tau^{-1}}{140p} + \frac{474}{497}\left(\frac{1}{p} - 1\right)\left(\frac{\tau^3}{6} + \frac{\tau^9}{135} + \frac{\tau^{15}}{600}\right)\right] / D$$

$$\Delta G_{chem\,(int)}^{\gamma\to\varepsilon} = RT\left[\chi_{N(bulk)} \ln\frac{\chi_{N(seg)}}{\chi_{N(bulk)}} + (1 - \chi_{N(bulk)})\ln\frac{1 - \chi_{N(seg)}}{1 - \chi_{N(bulk)}}\right]$$

$$\Delta G_{seg\,(int)}^{\gamma\to\varepsilon} = \Delta G_{chem\,(int)}^{\gamma\to\varepsilon} + \Delta G_{surf\,(int)}^{\gamma\to\varepsilon} + \Delta G_{el\,(int)}^{\gamma\to\varepsilon}$$

$$\Delta G_{surf\,(int)}^{\gamma\to\varepsilon} = \frac{1}{4}\Lambda(\chi_{N(seg)} - \chi_{n(bulk)})^2$$

$$\Delta G_{el\,(int)}^{\gamma\to\varepsilon} = \frac{2}{9}\mu\frac{1+\upsilon}{1-\upsilon}\left(\frac{dV}{dX}\right)\frac{1}{V}(\chi_{N(seg)} - \chi_{N(bulk)})$$

a: lattice parameter
a, b, c, d: coefficients
G_φ^Φ : Gibbs energy of pure elements
G_{mg}^Φ : magnetic contribution to Gibbs energy
${}^0L^\varphi$: linear function of T
${}^1L^\varphi$:constant
n: set of integers
N: Avogadro's constant
p: fraction of magnetic enthalpy absorbed above $T_{Néel}$
R: gas constant
$T_{Néel}$, T: (Néel) temperature

V: molar volume
β^Φ : magnetic moment
$\Delta G^{\gamma\to\varepsilon}, \Delta G_\varphi^{\gamma\to\varepsilon}, \Delta G_{mg}^{\gamma\to\varepsilon}$, $\Delta G_{seg\,(int)}^{\gamma\to\varepsilon}$ ($\Delta G_{chem(int)}^{\gamma\to\varepsilon}, \Delta G_{surf\,(int)}^{\gamma\to\varepsilon}$, $\Delta G_{el(int)}^{\gamma\to\varepsilon}$): change in Gibbs energy upon $\gamma - \varepsilon$ phase transformation, chemical, magnetic, and nitrogen segregation contributions (chemical, surface, elastic)

γ_{SFE}: stacking fault energy
μ: shear modulus
$\Omega_{\varphi\phi}^{\gamma\to\varepsilon}$: excess free energies
Λ : nitrogen atom-dislocation interaction energy
ρ: {111}molar surface density
σ: γ/ε-interface energy
ν: Poisson's ration
χ: molar fractions

Curtze, S., V. T. Kuokkala, A. Oikari, J. Talonen, and H. Hänninen. "Thermodynamic Modeling of the Stacking Fault Energy of Austenitic Steels." *Acta Materialia* 59, no. 3 (February 1, 2011): 1068–76. https://doi.org/10.1016/J.ACTAMAT.2010.10.037.

SFE, Temperature & Strain Rate Effects on Deformation Mechanism

- Competing $\dot{\varepsilon}$ effects
- High $\dot{\varepsilon}$ promotes twinning, but also raises T → suppresses twinning
- High $\dot{\varepsilon}$ also promotes HCP TRIP but not BCC

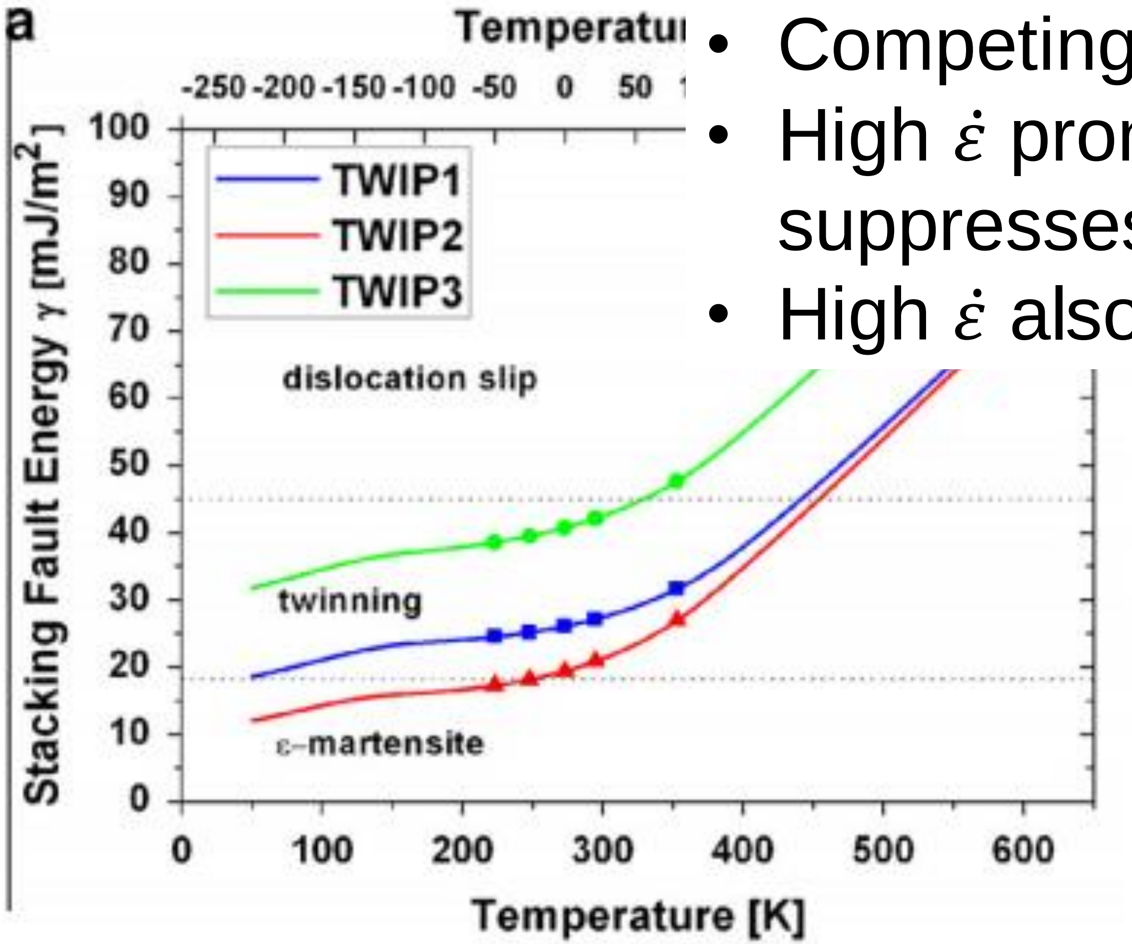

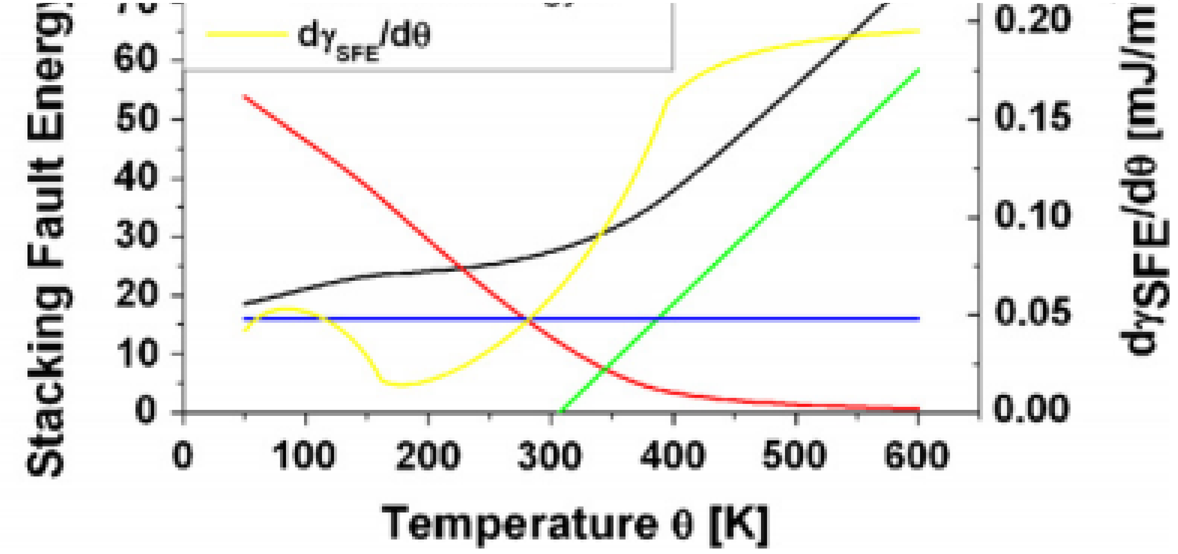

Curtze, S., and V. T. Kuokkala. "Dependence of Tensile Deformation Behavior of TWIP Steels on Stacking Fault Energy, Temperature and Strain Rate." *Acta Materialia* 58, no. 15 (September 1, 2010): 5129–41. https://doi.org/10.1016/J.ACTAMAT.2010.05.049.

Adiabatic Shear Banding & Microstructure

- Some evidence that aging affects ASB formation, morphology
- Zhang et al. (*J Mater Sci* June 2020) – ASBs in Al-Zn-Mg-Cu wider in overaged vs peak
- Wider ASB → higher critical strain/strain rate to form (Xue et al., *Acta* 44 1996)
- Peak age vs overage – different substructure in dynamic loading → diff shear localization behavior
- Torsion Kolsky best way to assess
- Also evidence of ASB dissolution of γ' (Colliander et al. *Phil Letters* Sept 2020)